Vertebrate Anatomy Morphology Palaeontology 1:1-21
ISSN 2292-1389

The postcranial skeleton of *Vagaceratops irvinensis* (Dinosauria, Ceratopsidae)

Robert B. Holmes
Department of Biological Sciences, University of Alberta, CW 405 Biological Sciences Building, Edmonton, Alberta, Canada T6G 2E9

Abstract: The postcranial skeleton of *Vagaceratops* (= *Chasmosaurus*) *irvinensis* (CMN 41357), lacking only the tail, most of the left front and left hind limbs, and portions of the pelvis, is preserved in articulation. It is one of the most complete, best articulated ceratopsid skeletons known. Both the manus and vertebral column exhibit conspicuous pathologies, possibly an indication of advanced age at the time of death. The vertebral column comprises a syncervical, six additional cervical vertebrae, and 12 dorsals. A partial synsacrum is represented by two dorsosacrals, four sacrals, two caudosacrals, and a partial third caudosacral centrum. The ribcage, although crushed, is nearly complete. The sternum is unusually wide compared with other ceratopsids. As in other chasmosaurines, the humerus bears a prominent deltopectoral crest that forms the anterior edge of the broad, rectangular proximal humeral expansion. The medial tuberosity is separated from the dorsal surface of the humerus by a distinct notch. The insertion for the latissimus dorsi is conspicuous. The deltopectoral crest extends a full half of the distance to the distal end of the humerus. Epipodials of the forelimb are relatively short compared to the corresponding propodial. The ulna has a long, distinctly triangular olecranon, broadly rounded anterolateral process, prominent medial process, and a deeply concave trochlear notch. The terminal phalanges on the fourth and fifth manual digits are relatively large, and unlike other ceratopsids have distinct distal (possibly articular) facets. The fourth trochanter of the femur is relatively proximal in position. This study and other recent studies of ceratopsid postcrania suggest that potentially useful taxonomic variation is present in the number of dorsosacrals, size of the groove on the ventral surface of the sacrum, morphology of the last dorsal and dorsosacral ribs, morphology of the scapula and proximal expansion of the humerus, morphology of the ulna, ratio of humerus/epipodium, morphology of the fifth manual digit, and position of the fourth trochanter of the femur.

Key Words: bone pathology, ceratopsid taxonomy, limb proportions, vertebral count variation

INTRODUCTION

The Ceratopsidae is a successful group of ornithischian dinosaurs that represented an important component of the Late Cretaceous terrestrial fauna of Laramidia, a landmass that formed the western shores of the Western Interior Seaway from what is now Alaska in the north to Mexico in the south (Sampson and Loewen 2010). These large-bodied quadrupeds are characterized by large skulls bearing prominent, posterodorsally directed frills and a variety of diagnostic horns, bosses and hooks. Two subfamilies, Centrosaurinae and Chasmosaurinae, are recognized principally on differences in the skull (see Dodson et al. 2004 for diagnoses).

The type of *Vagaceratops* (= *Chasmosaurus*) *irvinensis* (CMN 41357) was collected from sediments of the upper Dinosaur Park Formation near the town of Irvine in southern Alberta (see Holmes et al. 2001 for details). The specimen, consisting of an almost complete, articulated skeleton, is noteworthy in that when it expired, it came to rest in an approximately upright position, with its limbs tucked under its trunk. Preparation began in the late 1980s and continued sporadically throughout the 1990s as preparation time became available. The skull was eventually described, and an accompanying phylogenetic analysis placed the new species within the genus *Chasmosaurus* (Holmes et al. 2001). However, the generic placement of the species recently has been in flux. Sampson et al. (2010), in a subsequent analysis that incorporated new ceratopsid material and additional characters found it necessary to erect a new genus, *Vagaceratops*, to accommodate this taxon. Most recently, Longrich (2014), using a different data matrix has returned this species to *Chasmosaurus*. In this paper, the name *Vagaceratops* will be used, although it is recognized that the taxonomic placement of this species is subject to revision.

Preparation of the postcranial skeleton was not completed until 2003. Since then, the anatomy and function of the pectoral girdle and limb have been investigated (Thompson and Holmes 2007; Rega et al. 2010), and ossified tendons

Published 8 October 2014

submitted 11 March 2014; revisions received 2 September 2014; accepted September 16 2014.
Handling editor: Jordan Mallon.

associated with the vertebral column have been described (Holmes and Organ 2007), but otherwise the postcranium remains undocumented.

Phylogenetic analyses of ceratopsid interrelationships have traditionally been based overwhelmingly on cranial characters (e.g., Dodson et al. 2004; Currie et al. 2008; Sampson et al. 2010), presumably because articulated skeletons are rare. It has been suggested (Chinnery 2004; Maidment and Barrett 2011) that postcranial anatomy of ceratopsids is potentially informative, but this is difficult to assess because details of the postcranial anatomy of most ceratopsid taxa have not been described. As such, description of this largely complete postcranium provides much needed information on ceratopsid anatomy.

ABBREVIATIONS

Anatomical Abbreviations: acb, acetabulum; aceb, acetabular bar; acpr, acromion process; alpr, anterolateral process of the ulna; ast, astragalus; atc, centrum of atlas; axc, centrum of axis; axrart, articulations for axis rib; axsp, neural spine of axis; c3, third carpal; c4, fourth carpal; C4–C9, fourth–ninth cervical vertebrae; C3art, articulation for third cervical rib; C3cent, centrum of thord cervical vertebra; C3sp, neural spine of third cervical vertebra; cal, calcaneum; CS1–CS4, first–fourth caudoscral vertebrae; dpcr, deltopectoral crest; D1–D12, first–twelfth dorsal vertebrae; DS1, first dorsosacral vertebra; DS2, second dorsosacral vertebra; dsc, ridge for insertion of dorsalis scapulae; fibc, fibular condyle of tibia; gl, glenoid; gr, midventral groove on sacrum; hh, humeral head; ilpr, iliac process of ischium; lcor, left coracoid; ld, insertion of the latissimus dorsi; lfem, left femur; lhum, left humerus; lisc, left ischium; lpub, left pubis; lscap, left scapula; lst, left sternal plate; mc1, first metacarpal; mc5, fifth metacarpal; mpr, medial process of ulna; mt5, fifth metatarsal; mtub, medial tuberosity; n, notch separating medial tuberosity from dorsal surface of proximal humeral expansion; ob, obturator foramen; ol, olecranon; paraC9, parapophysis on the ninth cervical vertebra; paraD1, parapophysis of first dorsal vertebra; path, pathological bone; ph1, proximal phalanx of first manual digit; ppr, pubic process of ischium; pprpub, posterior process of pubis; pub, prepubic process; rC3−rC9, third−nineth cervical ribs; rD1−rD12, first−twelfth dorsal ribs; rDS1, first dorsosacral rib; rfem, right femur; rfib, right fibula; rhum, right humerus; risc, right ischium; rpes, right pes; rpub, right pubis; rrad, right radius; rscap, right scapula; rst, right sternal plate; rtib, right tibia; rul, right ulna; S1–S4, first–fourth sacral vertebrae; sac, sacrum; sccsut, scapulocoracoid suture; sglb, supraglenoid buttress; shisc, shaft of ischium; spn1, spinal nerve passing between atlas and axis; spn2, spinal nerve passing between axis and third cervical; sr1–sr4, first–fourth sacral ribs; t?, possible tarsal element; tp5, terminal phalanx of fifth manual digit; tprDS2, transverse process of second dorsosacral vertebra; tr4, fourth trochanter; trf, triceps fossa.

Institutional Abbreviations: CMN, Canadian Museum of Nature, Ottawa, ON, Canada; YPM, Yale Peabody Museum, New Haven, CT, USA; ROM, Royal Ontario Museum, Toronto, ON, Canada.

DESCRIPTION

Although CMN 41357 has suffered some dorsoventral compression, and weathering has damaged or destroyed the tail and some bones on the left side of the body, the skeleton represents one of the most complete ceratopsid skeletons ever discovered. Most of the bones are preserved either in articulation or close to their natural positions, leaving no doubt as to their mutual relationships. CMN 41357 therefore provides much important information on the structure and organization of the ceratopsid skeleton. Although some elements of the skeleton are distorted, many useful measurements were obtained (Appendix 1).

Vertebral Column and Ribs

The presacral vertebral column, composed of the syncervical, six additional cervicals, and 12 dorsals, is 1455 mm in length. During burial, the skull, syncervical, and fourth cervical drifted a short distance from the rest of the skeleton, but are still preserved in close association with the remainder of the cervical series. The remainder of the presacral column, including the fifth−ninth cervicals and 12 dorsals, are preserved in articulation (Fig. 1). The synsacrum, composed of two dorsosacrals, four sacrals, two caudosacrals and a partial third caudosacral still lies in its natural position (Fig. 1). The remainder of the synsacrum and caudal vertebrae were lost to weathering and erosion before the skeleton was collected. As a consequence of pathologies and/or extensive dorsoventral compression (see below), it is not possible to obtain meaningful measurements of many vertebral dimensions.

The rib cage is nearly complete, although dorsoventral compression of the skeleton during sediment compaction has resulted in breakage and deformation of most elements. Except in the anterior cervical region, each rib is preserved in close association with its respective vertebra (Fig. 1), permitting unequivocal identification of nearly all ribs (Fig. 2).

Cervical Vertebrae and Ribs: The syncervical is nearly complete, missing only the atlas arches and portions of the dorsal margin of the axis spine (Fig. 3). Its morphology is similar to that of other ceratopsids. The delicate rim of the anterior cotyle of the atlas is damaged, but otherwise the centra are well preserved, and clearly exhibit the tripartite composition of the ceratopsid syncervical (Campione

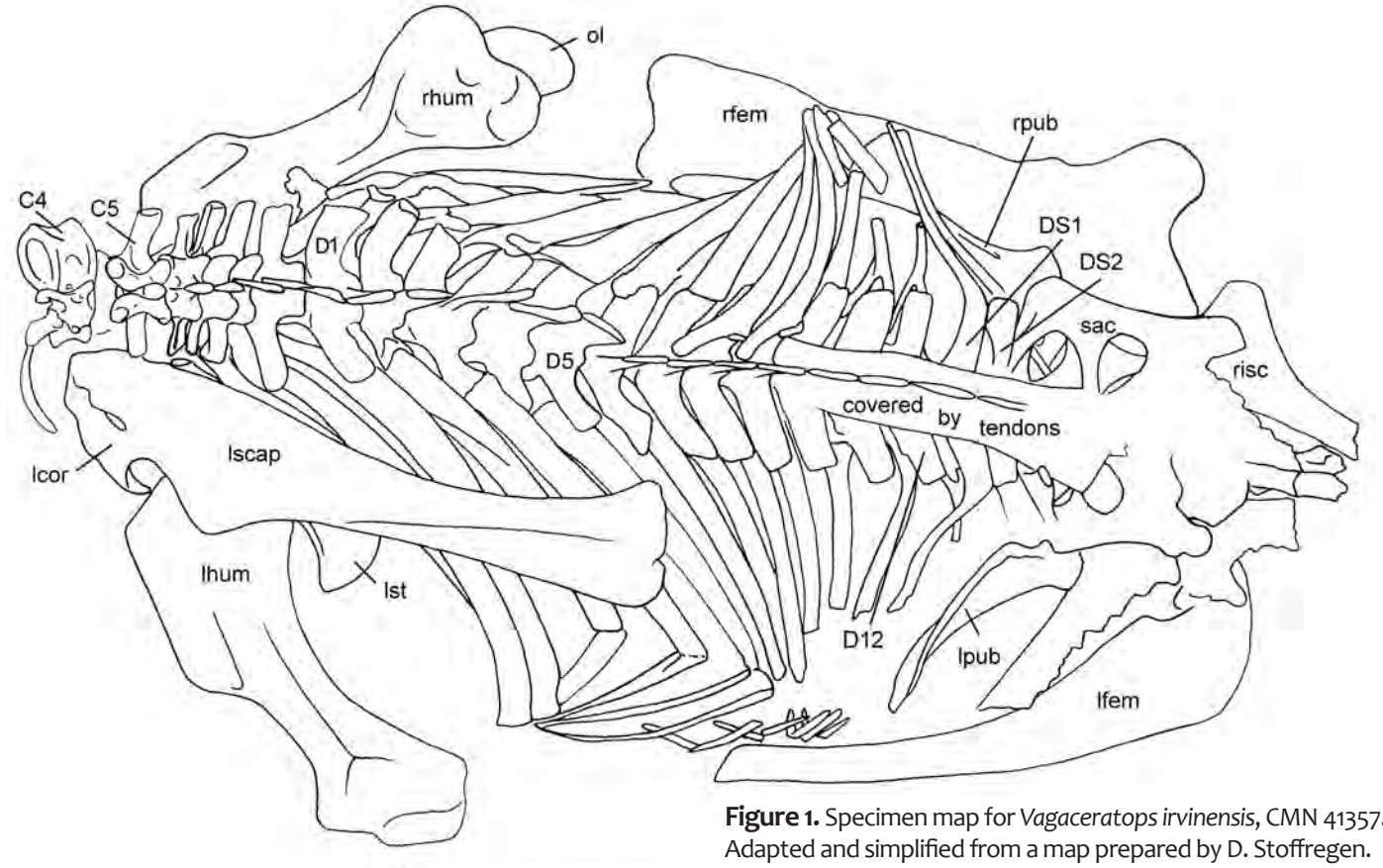

Figure 1. Specimen map for *Vagaceratops irvinensis*, CMN 41357. Adapted and simplified from a map prepared by D. Stoffregen.

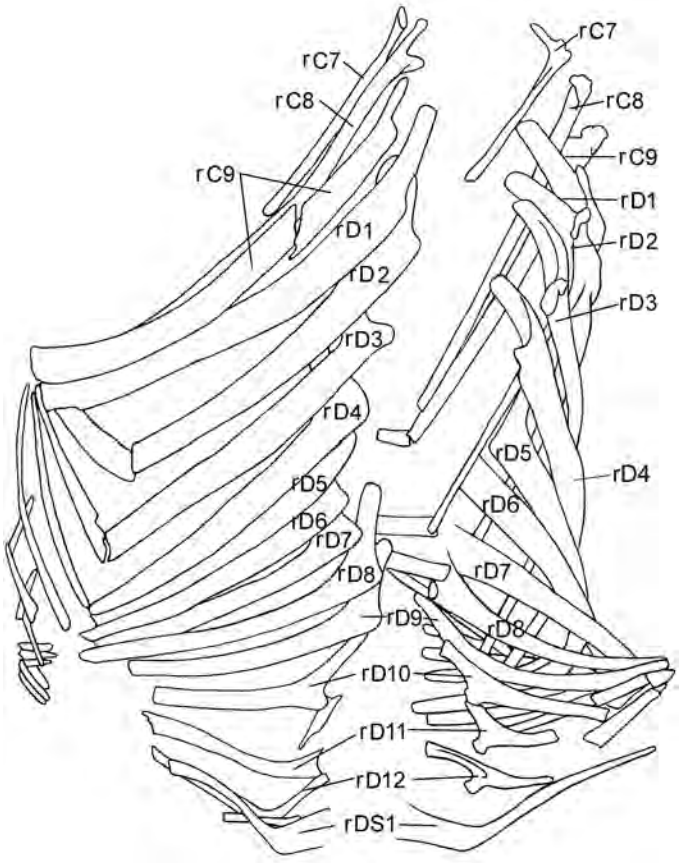

Figure 2. Specimen map showing relative position of ribs. *Vagaceratops irvinensis*, CMN 41357. Adapted and simplified from a map prepared by D. Stoffregen.

and Holmes 2006; Tsuihiji and Makovicky 2007). The combined centra are 296 mm in length, and the posterior face of the last centrum is 115 mm high and 89 mm wide. The posterior margin of the slit-shaped canal for the spinal nerve passing between the atlas and axis, as well as the large oval foramen for the passage of the spinal nerve between the axis and third cervical vertebra are clearly visible. Diapophyses and parapophyses of both the axis and third cervical vertebra are preserved. As in other ceratopsids except possibly *Arrhinoceratops* (Mallon et al. 2014), there is no evidence of atlantal rib attachments.

The fourth cervical was removed from the block and prepared in three dimensions (Fig. 4). It closely resembles that of *Styracosaurus* (Holmes and Ryan 2013) in the possession of a short, stout neural spine, and short laterally and slightly ventrally directed transverse processes. Its centrum is 106 mm wide and 69 mm long. As in other ceratopsids (e.g., Maidment and Barrett 2011; Holmes and Ryan 2013), the centrum is heart-shaped in anterior view. Although the center of the anterior articular surface is slightly concave, the centrum is essentially amphiplatyan. Cervicals 5–8 show a number of pathological features (Fig. 5). The fifth cervical has fused to the sixth cervical, but otherwise appears normal. The total length of the co-ossified centra of cervicals 6–8 is only about twice that of the centrum of the fifth cervical (131 mm as compared to 65 mm), mostly as a result of the collapse of the centrum of the eighth vertebra. The left lateral

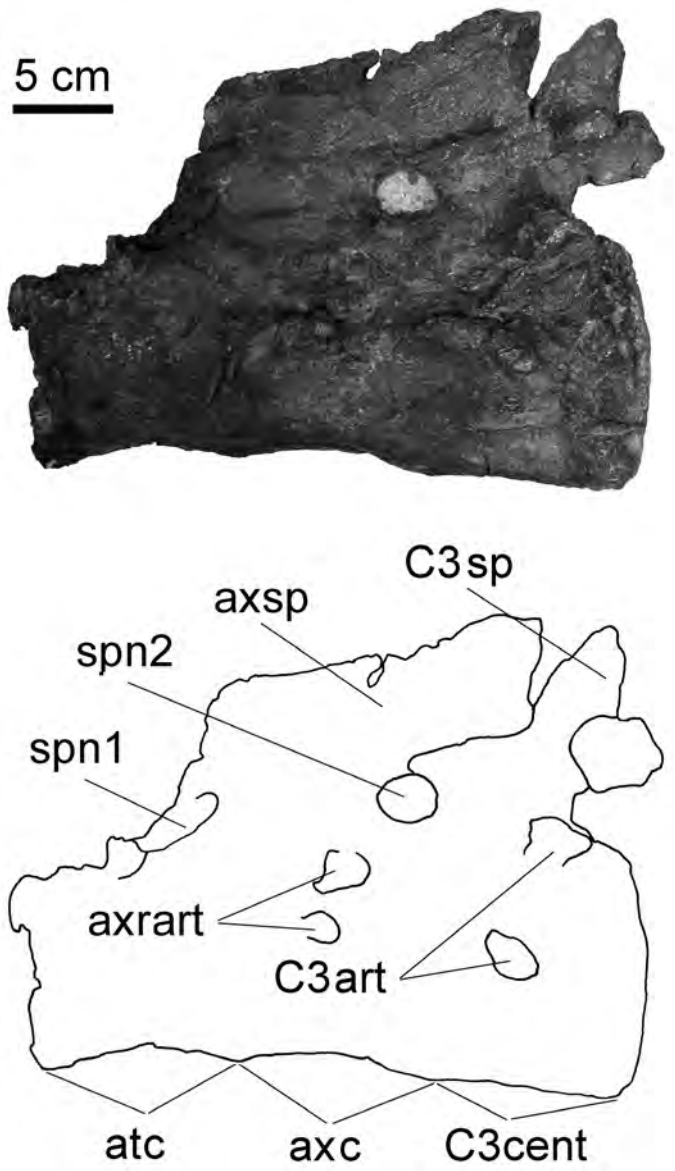

Figure 3. Syncervical in left lateral view. *Vagaceratops irvinensis*, CMN 41357.

surfaces of the vertebrae are covered with cauliflower-shaped growths. At least one pathology has been reported in the cervical region of ceratopsids (Lull 1933), but this is limited to simple fusion of two vertebrae of otherwise normal appearance. The centrum of the ninth cervical is articulated closely

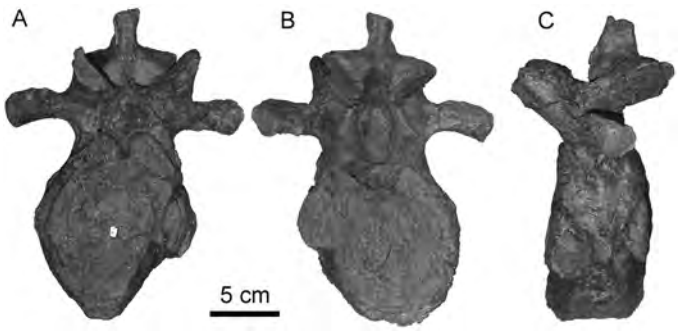

Figure 4. Fourth cervical in anterior, posterior, and left lateral views. *Vagaceratops irvinensis*, CMN 41357.

to that of C8, to which it may be fused, but otherwise, this vertebra exhibits no obvious abnormalities.

On the right side, the rib associated with C3 (i.e., last segment of the syncervical) is complete and undistorted (Fig. 6). The tuberculum and capitulum are connected by a broad web of bone bearing a blunt, anteriorly-projecting prong. A short, pointed, spine-like rib shaft projects from the posterior edge of the rib body. The tuberculum is missing from rib C4, but a capitulum and distinct, blunt, posteriorly-directed shaft are preserved (Fig. 6). Rib C5 bears a dorsally curved shaft. Rib C6 could not be identified. The ribs associated with the syncervical and fourth cervical are missing on the left side. The left ribs of C5 and C6 are preserved in their natural positions, but are deformed, swollen, and much shorter than their equivalents on the right side (Fig. 5). Ribs associated with vertebrae C7–C9 are preserved on both sides (Fig. 2). The shaft of rib C7 (Fig. 7) is much longer than that of C5, but as rib C6 is missing from the right side, and is badly deformed on the left side, it is uncertain whether there is a gradual or abrupt lengthening of the shaft in this region of the neck. The left ribs associated with C7–C9 are complete and show relatively little distortion (Fig. 7). Rib C7 is almost straight and tapers to a blunt point distally. Rib C8 is gently curved ventrolaterally and distinctly longer than rib C7. Rib C9, bears a stout shaft that is expanded distally, suggesting that it extended as a sternal cartilage in life.

Dorsal Vertebrae and Ribs: Twelve dorsal vertebrae are preserved in articulation (Fig. 1), but were separated into two segments during preparation (Figs. 8, 9). Their centra were strongly compressed dorsoventrally during preservation, but unlike the cervical vertebrae, do not exhibit any obvious pathologies or other abnormalities. A well-developed tendon trellis (Holmes and Organ 2007) covers the bases of the neural arches and obscures most of the zygapophyses. As in other ceratopsids, the transverse processes of the anterior dorsal vertebrae project approximately 90° from the axis of the column, and are directed slightly dorsally. They become progressively more posteriorly and dorsally inclined toward the posterior end of the series. The anteroposteriorly broad, blade-like neural spines become more elongate toward the sacrum. The neural spine and postzygapophyses of the last dorsal vertebra (D12) appear to be fused to that of the first dorsosacral, but the centra of these two vertebrae show no evidence of co-ossification, as in one specimen of *Centrosaurus* (YPM 2015, Lull 1933).

All ribs of the dorsal series (D1–D12) are preserved (Fig. 2). Ribs on the left side (Figs. 7, 10) are less distorted. In contrast with the preserved cervical ribs, which are distinctly bifurcated proximally to support the widely separated tubercular and capitular facets (Figs. 6, 7), tubercular processes are reduced in the dorsal ribs, and the tubercular

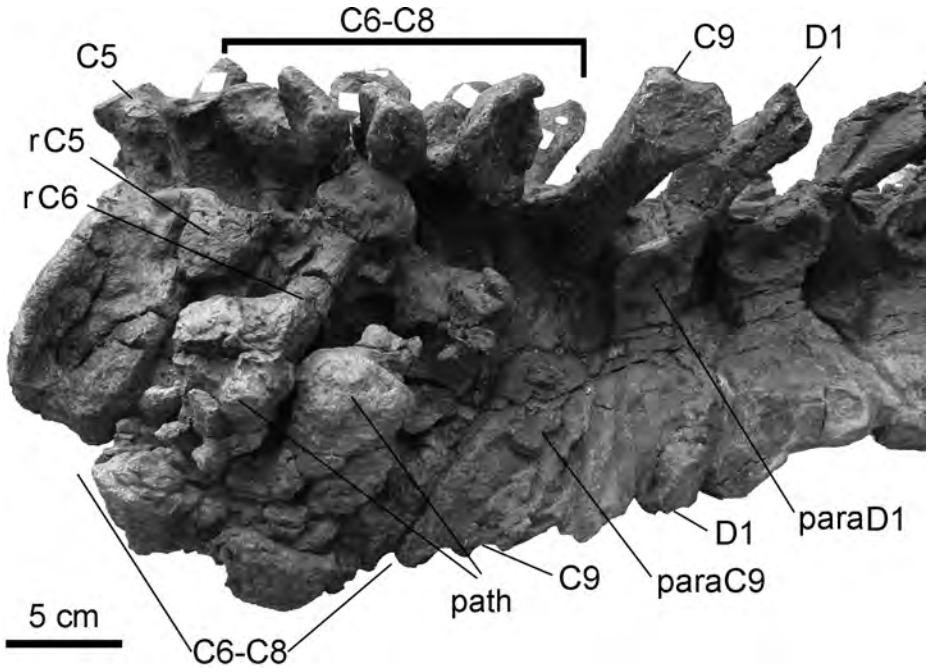

Figure 5. Left aspect of cervical vertebrae showing abnormalities. *Vagaceratops irvinensis*, CMN 41357.

facets for articulation with the diapophyses are born on the dorsal surfaces of the rib angles (Figs. 7, 10). The first two dorsal ribs bear expanded distal ends suggesting that they were extended in sternal cartilages in life (Fig. 7). All other ribs from the left side sustained damage as the rib cage was compressed dorsoventrally during sediment compaction. The distal ends in most cases have separated from their proximal counterparts and have come to rest a short distance ventrolaterally from their natural positions (Fig. 2). All taper distally, or end bluntly without expansion, indicating that none were extended as sternal cartilages.

The dorsal ribs on the right side have suffered diagenetic compression. Ribs D1–D5 are complete, but are broken about 2/3 down the shaft and torqued (Fig. 2). Ribs D6–D11 are generally complete and undistorted proximally, but as on the left side, their distal ends have become separated and have clustered in a densely compacted mass under the proximal shafts of D8–D11. Nevertheless, their relative spatial relationships have been preserved, and each rib end can be associated with its proximal half.

Figure 6. Cervical ribs C3–C5, right side. *Vagaceratops irvinensis*, CMN 41357.

Synsacrum

The incomplete synsacrum includes two dorsosacrals, four sacral vertebrae bearing stout sacral ribs ('parapophyses' of Hatcher et al., 1907 and Lull, 1933), two complete caudosacrals, and the anterior half of the third caudosacral (Figs. 9, 11). The dorsal portions of all sacral and caudosacral vertebrae are poorly preserved, and the neural spines are missing.

Dorsosacral Vertebrae and Ribs: The centra of the two dorsosacrals are co-ossified, but the position of the articulation between the two centra is clearly visible. Each centrum measures approximately 65 mm anteroposteriorly, comparable in length to centra of the posterior dorsal vertebrae. The transverse processes of the first dorsosacral vertebra project almost directly laterally and bear co-ossified ribs. The second dorsosacral bears blade-like, laterally projecting transverse processes. They are only a few millimeters thick at their posterior margin and taper to a sharp edge anteriorly. Each transverse process is anteroposteriorly flared at its distal end. There is no evidence of a terminal rib attachment—as in other ceratopsids, the transverse process probably articulated with the inner dorsal margin of the ilium, but because neither ilium is preserved, this cannot be confirmed.

The ribs associated with the first dorsosacral (the 22nd vertebra) are distinct from the more anterior ribs in the complete absence of a ventral articulation (capitulum) and fusion of the dorsal articulation (tuberculum) to the diapophysis of the transverse process. The dorsoventrally flattened, nearly straight, blade-like rib shaft projects anterolaterally (Fig. 9). A similar rib has been described in association with the twelfth dorsal vertebra in *Centrosaurus* (Lull 1933:fig. 18), but in contrast with CMN 41357, it seems to retain a well-developed capitular process, and appears to have lost its association with the diapophysis of the transverse process. Rather than articulating with the rib, the transverse process articulates with the dorsomedial edge of the ilium as they do in more posterior sacral vertebrae.

Sacral Vertebrae and Ribs: Each sacral centrum is approximately 90 mm in length, considerably longer than those of the dorsal and dorsosacral vertebrae, each of which is approximately 65—70 mm in length. Each sacral vertebra bears a pair of sacral ribs that project from the lateral surfaces of the centrum (Figs. 9, 11). As in other ceratopsids, the first pair of ribs is by far the most massive. The broad base of each rib appears to spread anteroposteriorly across the entire lateral surface of the centrum and may

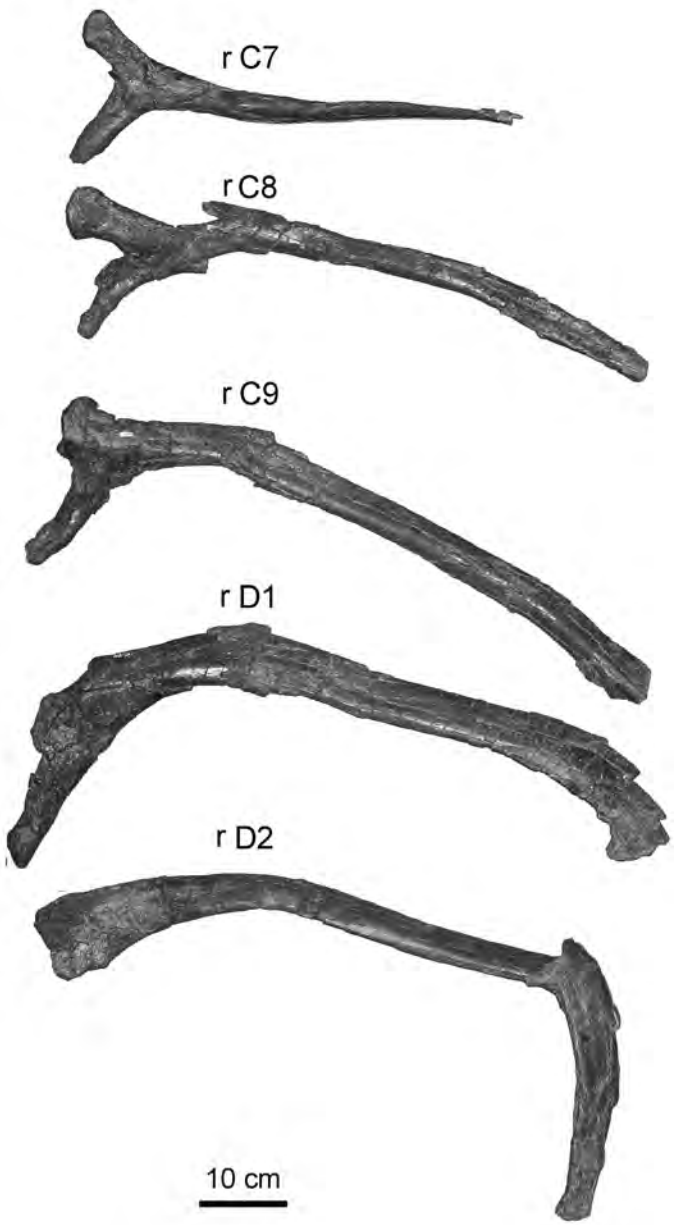

Figure 7. Ribs C7–C9, D1, D2, left side. *Vagaceratops irvinensis*, CMN 41357.

have encroached onto the adjacent centra, although the extent to which this occurs cannot be confirmed because the vertebrae in this part of the synsacrum are almost indistinguishably co-ossified. These ribs project posterolaterally, and expand distally to form the anterior portion of the buttress supporting the medial surface of the acetabular bar. A partial transverse process ('diapophysis' of Hatcher et al. 1907 and Lull 1933) is preserved only on the left side of the first sacral vertebra. A bony septum originating from the dorsal surface of the sacral rib sweeps posterodorsally to support the underside of this transverse process. The less massive second sacral ribs project laterally, and only slightly posteriorly, but are otherwise similar to the first sacral ribs. Distally, each expands to contribute significantly to the buttress for the acetabular bar. As with the first two sacral vertebrae, the third and fourth sacral vertebrae are co-ossified, but the suture is visible. Both bear the bases of sacral ribs, but only the left rib on the third vertebra is complete. Transverse processes and neural spines of both vertebrae are missing. A median groove is clearly present on the ventral surface of the sacrum. It is best developed on the second sacral vertebra, and becomes shallower as it extends anteriorly and posteriorly onto the ventral surface of the first and third sacral vertebrae, respectively (Fig. 11). At present, it cannot be described in more detail because the specimen is mounted for public display, and cannot be accessed.

Caudosacral Vertebrae and Ribs: Two caudosacral centra and the anterior portion of a third are co-ossified to the posterior end of the sacrum. They are noticeably narrower and less massive than the sacral vertebrae, and are distinctly constricted at mid-length. A similar morphology is present in the caudosacrals of *Chasmosaurus belli* (ROM 843, Fig. 12) and the anterior-most caudal vertebrae in *Styracosaurus* (Holmes and Ryan 2013). The neural arches and transverse processes are missing, exposing the neural canal dorsally.

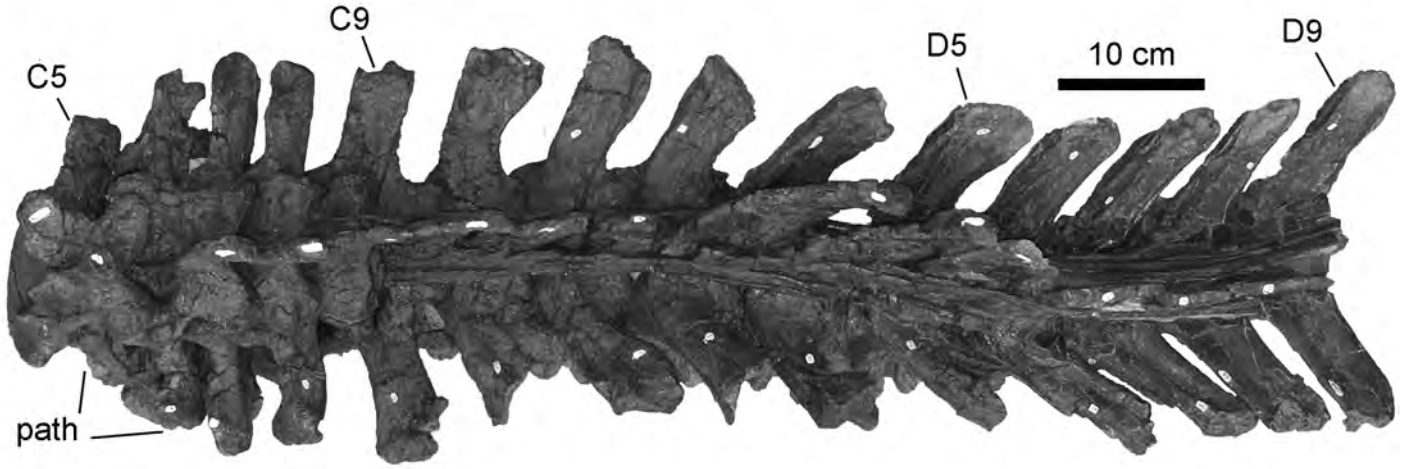

Figure 8. Cervical vertebra five to dorsal vertebra 9, in dorsal view. *Vagaceratops irvinensis*, CMN 41357.

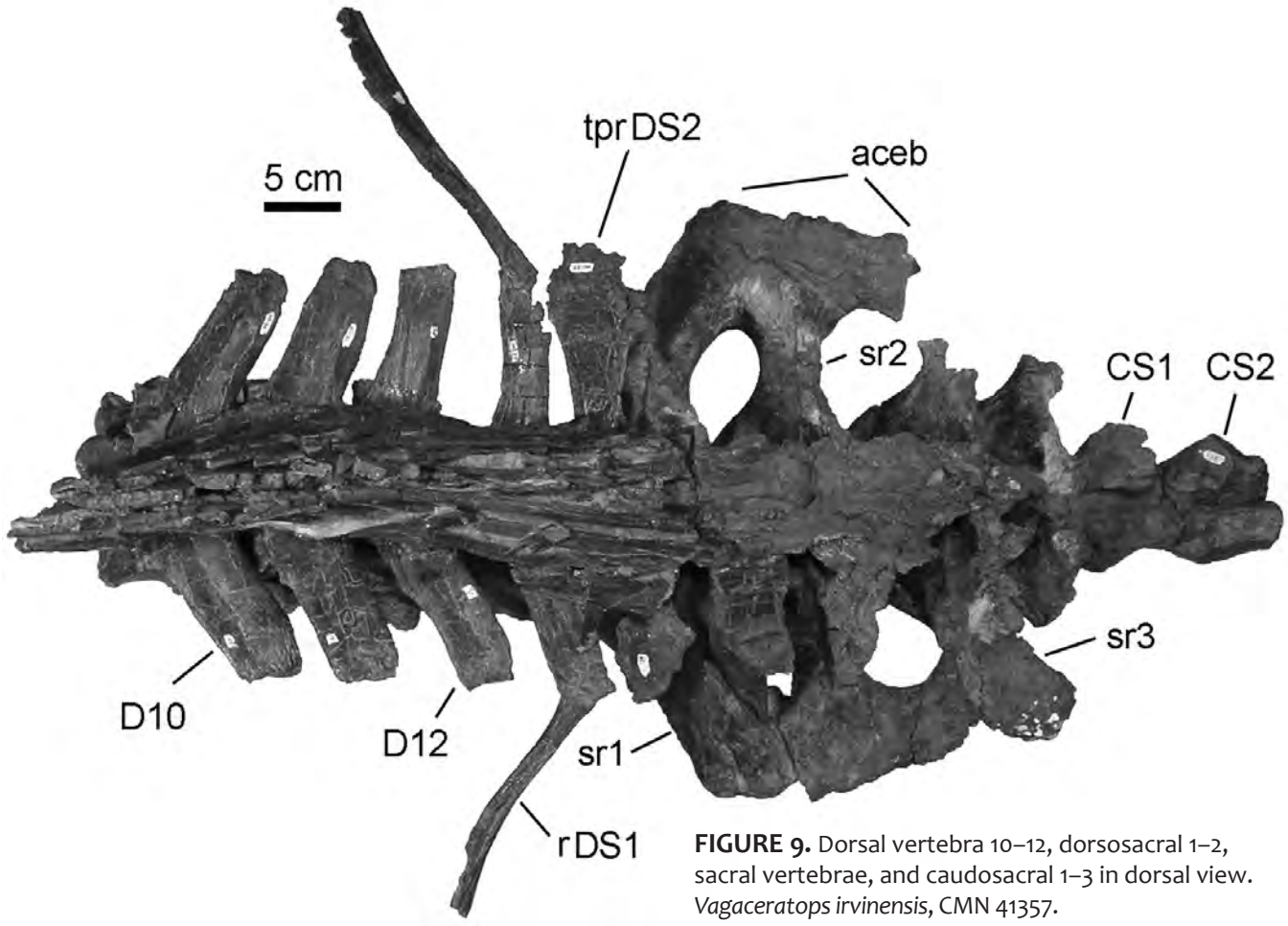

FIGURE 9. Dorsal vertebra 10–12, dorsosacral 1–2, sacral vertebrae, and caudosacral 1–3 in dorsal view. *Vagaceratops irvinensis*, CMN 41357.

Pectoral Girdle and Limb

Both scapulae are preserved in place (Figs. 1, 13). The left scapula is complete and essentially undistorted (Fig. 14B). The indistinct acromion process forms a gentle convexity along much of the anterior margin of the scapular blade. This is distinct from the condition in centrosaurines, in which the process is localized to a small area immediately distal to the scapulocoracoid suture (Maidment and Barrett 2011. A more extensive acromion process may be a chasmosaurine character (Maidment and Barrett 2011). A thick ridge, presumably associated with the origin of the dorsalis scapulae muscle (Johnson and Ostrom 1995) arises on the proximo-ventral corner of the scapula as the glenoid buttress, passes diagonally across the lateral surface of the blade, and subsides near the dorsal margin of the scapula at approximately the midpoint between the scapulocoracoid suture and the distal end of the blade. This resembles the condition in *Centrosaurus* (Lull 1933), *Styracosaurus* (Holmes and Ryan 2014), cf. *Anchiceratops* (Mallon and Holmes 2010), and *Chasmosaurus* (RH, pers. obs., although there appears to be some variability in the course of the ridge in the latter genus), but is distinct from the condition in *Triceratops* (Hatcher et al. 1907) and *Torosaurus* (Johnson and Ostrom 1995), in which the ridge terminates posteriorly midway between the dorsal and ventral margins of the blade. Both coracoids are preserved and essentially complete, but were folded under the body during dorsoventral compression of the carcass, obscuring details of the scapulocoracoid suture and coracoid foramen. The supracoracoideus scar is poorly developed.

Sternal Plates: Sternal plates are preserved in approximately natural position (Fig. 13). The ventral (external) surface of each plate (Fig. 15A) bears a low, broad, longitudinal ridge that parallels its thickened lateral border, much as in *Centrosaurus* (see Brown 1917:fig. 3). The dorsal (internal) surface (Fig. 15B) is slightly concave. Its curved anterior border bears a rugose surface for articulation with the posterior margin of the coracoid. The lateral margin of each plate curves strongly laterally toward its posterior end, creating a very wide sternum in comparison to those described in *Centrosaurus* (Brown 1917; Lull 1933), *Styracosaurus* (Holmes and Ryan 2013) and *Triceratops* (Brown 1906). Its thickened, curved posterior margin bears a series of crenulations where sternal cartilages of ribs presumably attached, although as in *Styracosaurus* (Holmes and Ryan 2013), specific attachment points cannot be identified.

Figure 10. Ribs D3–D12, left side. *Vagaceratops irvinensis*, CMN 41357.

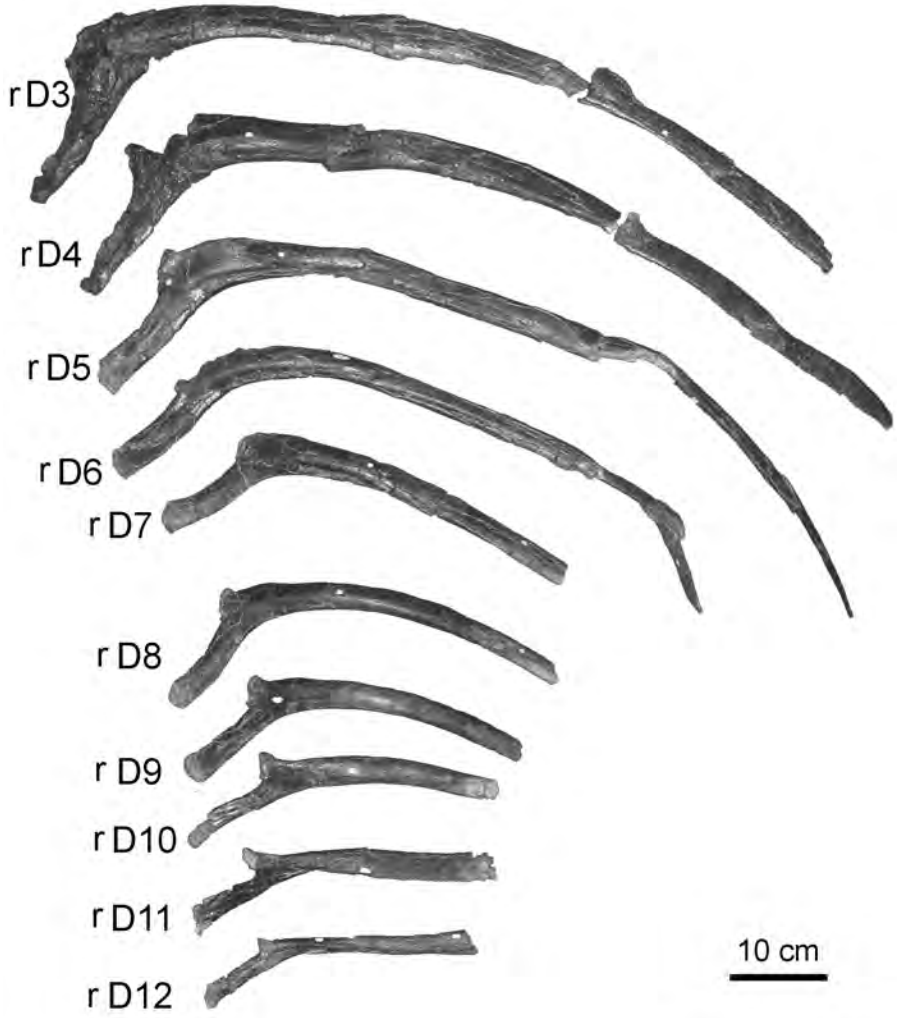

Humerus: Both humeri are preserved (Figs. 1, 16). The right humerus (Fig. 17) is essentially complete, and although somewhat flattened, is otherwise undistorted. It comprises a short shaft connecting broad proximal and distal expansions. Its proximal expansion is large and rectangular in outline, with a straight preaxial deltopectoral crest that terminates distally in a conspicuous rugosity for the insertion of the pectoralis musculature. This morphology is, as far as known, characteristic of chasmosaurines (Hatcher et al. 1907:fig. 65; Johnson and Ostrom 1995:fig. 12.3; Lehman 1998:fig. 4; Mallon and Holmes 2010:fig. 13.6; Maidment and Barrett 2011:fig. 23), but distinct from the morphology seen in centrosaurines (Lull 1933:fig. 21; Holmes and Ryan 2013), in which the proximal humeral expansion is less broad, the preaxial border of the deltopectoral crest is distinctly concave in outline, and the pectoralis insertion is more proximal in position (Maidment and Barrett 2011). The dorsal surface of each humerus bears a longitudinal groove on the posterodistal corner of the proximal expansion. Although crushing has obscured its morphology, there appears to be a foramen at the distal end of the groove on the left humerus. This feature, probably marking the insertion of the latissimus dorsi, is better developed in chasmosaurines than in centrosaurines (Maidment and Barrett, 2011). The humeral head has been crushed, but its outline is clear. Lateral to the condyle, on the extensor surface of the proximal expansion, the humerus bears a shallow triceps fossa. A deep triceps fossa is believed to be characteristic of chasmosaurines (Maidment and Barrett 2011), but both humeri of CMN 41357 were dorsoventrally compressed during preservation, so the original depth of this fossa cannot be determined. As in other chasmosaurines, but not centrosaurines (Maidment and Barrett 2011), the medial tuberosity is set off from the dorsal surface of the humerus by a distinct notch. The humeral shaft is short (a consequence of the large proximal expansion and distal placement of the pectoralis insertion) and the distal humeral expansion appears to be relatively broad in comparison with the condition seen in centrosaurines (e.g., Holmes and Ryan 2013), although this impression may be the result of dorsoventral crushing.

Ulna: The right ulna is well preserved (Fig. 17). The olecranon is well developed, although it is distinctly triangular in shape rather than rounded as in most ceratopsids. The precise length of the process is difficult to measure because the proximal limit of the articular facet for the humerus cannot be located precisely. However, a proxy for the process lenght was made by measuring the distance from the distal margin of the articular facet to the tip of the process and dividing this by the total length of the ulna. This gives the following ratios: CMN 41357, 0.34; *Triceratops* (Hatcher et al. 1907), 0.44; *Torosaurus* (Johnson and Ostrom 1995), 0.35; cf. *Anchiceratops* (Mallon and Holmes 2010, 0.40, *Chasmosaurus* (Maidment and Barrett 2011), 0.30; *Pentaceratops* (Wiman, 1930), 0.29; *Centrosaurus* (Lull 1933), 0.34; *Styracosaurus* (Holmes and Ryan 2013), 0.29. The ratio in CMN 41357 is close to the average value for chasmosaurines. *Centrosaurus* and *Styracosaurus* exhibit relatively low values, lending support to the suggestion that centrosaurines have a shorter olecranon than chasmosaurines (Adams 1988 in Dodson et al., 2004), although it should be kept in mind that both

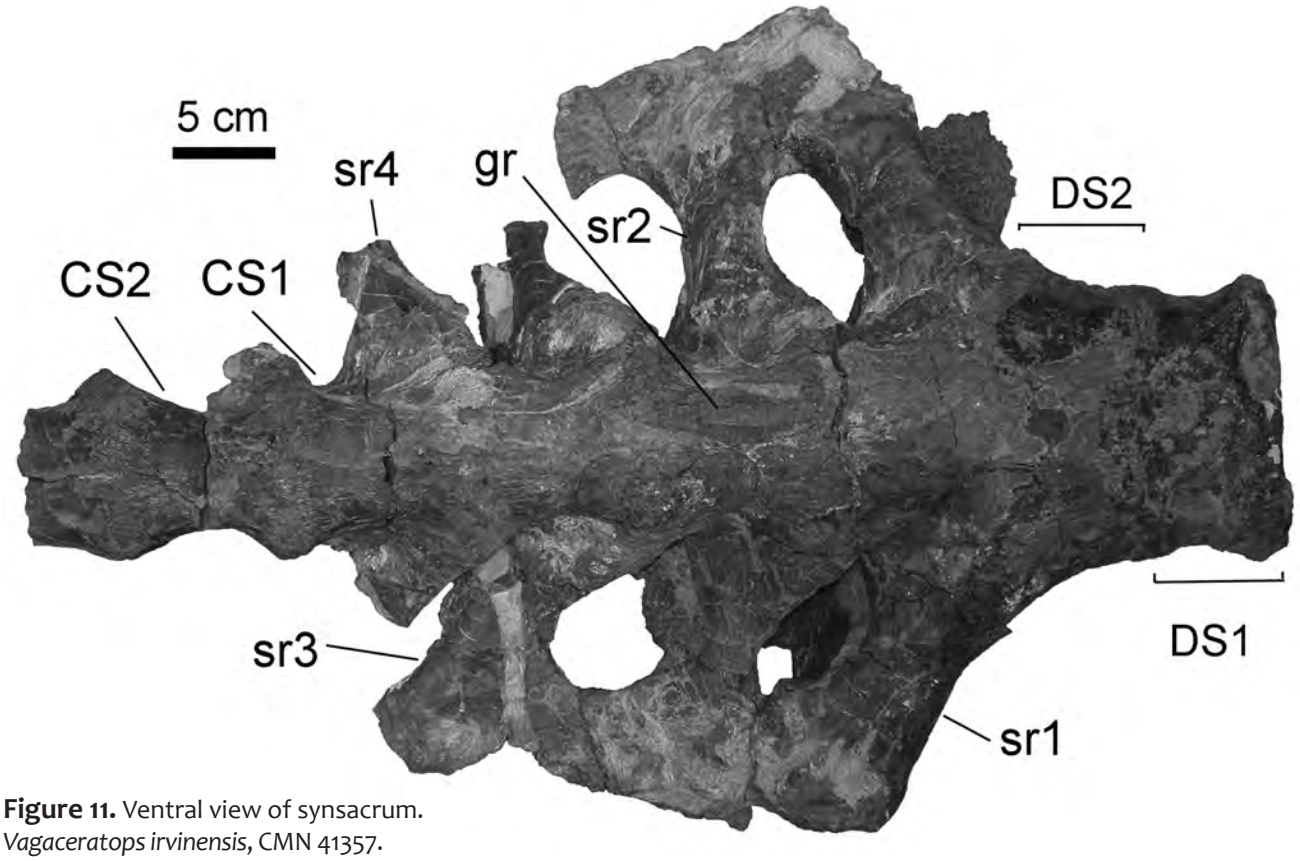

Figure 11. Ventral view of synsacrum. *Vagaceratops irvinensis*, CMN 41357.

Chasmosaurus and *Pentaceratops* overlap the centrosaurine range, which suggests the possibility that olecranon length is a variable character in ceratopsids and therefore of no taxonomic significance.

The anterolateral process of the ulna does not present a triangular outline as it does in *Chasmosaurus* (Maidment and Barrett 2011) and *Pentaceratops* (Wiman 1930:plate 6), but rather forms a broadly rounded crest that extends for a considerable distance onto the lateral surface of the olecranon. The medial process is very prominent, and the proximal articulation for the humerus (trochlear notch) is deeply concave, much as reported in other chasmosaurines such as *Chasmosaurus* (Maidment and Barrett 2011:fig. 24), *Pentaceratops* (Wiman, 1930:pl. 6), *Triceratops* (Hatcher et al. 1907:fig. 67), and *Torosaurus* (Johnson and Ostrom 1995:fig. 12.6), In centrosaurines as far as known, the median process is relatively shorter, and the trochlear notch is much less concave (Lull 1933:fig. 22; Holmes and Ryan 2013:fig. 20; Gilmore 1917:fig. 35), a configuration that appears to be accentuated by the relatively short olecranon, at least in these described specimens.

Radius: The radius (Fig. 17) is modestly expanded at both ends. As in other ceratopsids, the proximal articular surface exhibits a compressed oval outline with a shallow central concavity to accommodate the radial condyle of the humerus. The distal expansion bears a long narrow articular surface for the carpus.

The ratio of radius length (340 mm) to humerus length (610 mm) is 0.56 if the latter is measured to the distal end of the radial condyle. This is slightly less than the ratio of 0.57 in cf. *Anchiceratops*, 0.58 in *Styracosaurus*, and 0.58 in *Centrosaurus*, and considerably less than 0.67 in *Pentaceratops* (Wiman 1930), and 0.62 in *Triceratops* (Fujiwara 2009).

Carpus, Metacarpus, and Manus: Upon death, the carcass settled in an upright position. The right epipodials were folded under the right humerus, and right carpus, metacarpus, and manus came to be exposed with the ventral (flexor) aspect turned dorsally (Fig. 16). As in other ceratopsids, only two carpal elements, probably distal carpals 3 and 4, ossified. The fourth is slightly larger. The manus is preserved in close association except for the phalanges of digits 4 and 5, which had drifted a short distance from the other bones. All elements are well-preserved, although the metacarpal and proximal phalanx of the first digit exhibits pathological bone growth (Fig. 18; Rega et al. 2010, fig. 24.1), a condition hypothesized to be the result of repetitive stress induced by toe jamming associated with the unique rolling gait of ceratopsids (Rega et al. 2010). The first metacarpal is deformed to the point that it is impossible to distinguish the dorsal and ventral surfaces. Since all elements of the right manus, including the terminal phalanx and probably first phalanx of the first digit, were preserved with their ventral aspect facing upward, it was originally assumed that the first metacarpal

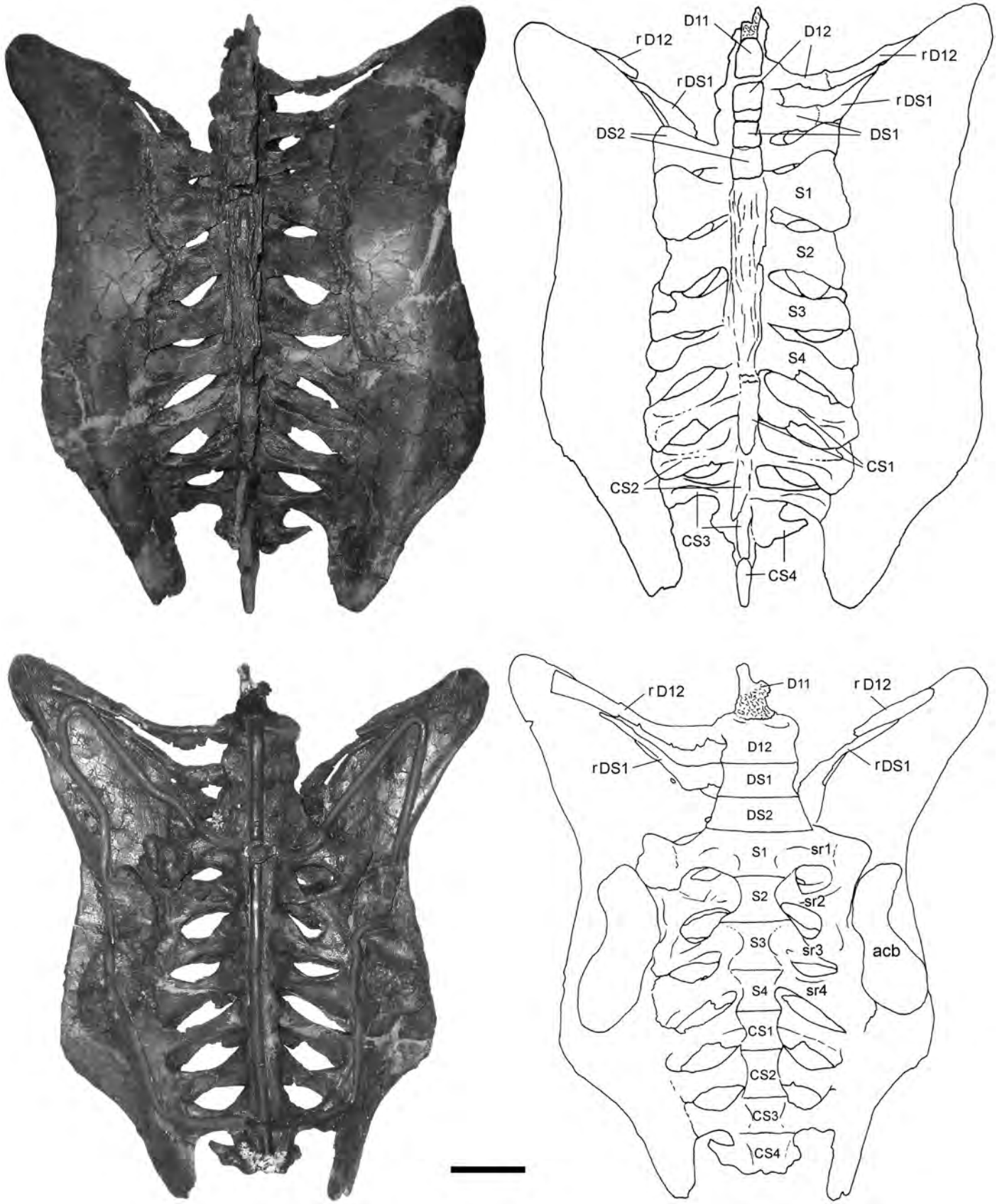

Figure 12. Synsacrum and pelvis of *Chasmosaurus belli* (ROM 843) in dorsal (upper) and ventral (lower) views. The neural spine (but not the arch or the centrum) of the 11th dorsal vertabra is preserved in articulation with the last (12th) dorsal vertebra. The latter has fused to the front of the synsacrum. Two dorsosacrals, each with almost completely co-ossified dorsoventrally flattened ribs lacking capitular processes, are present.

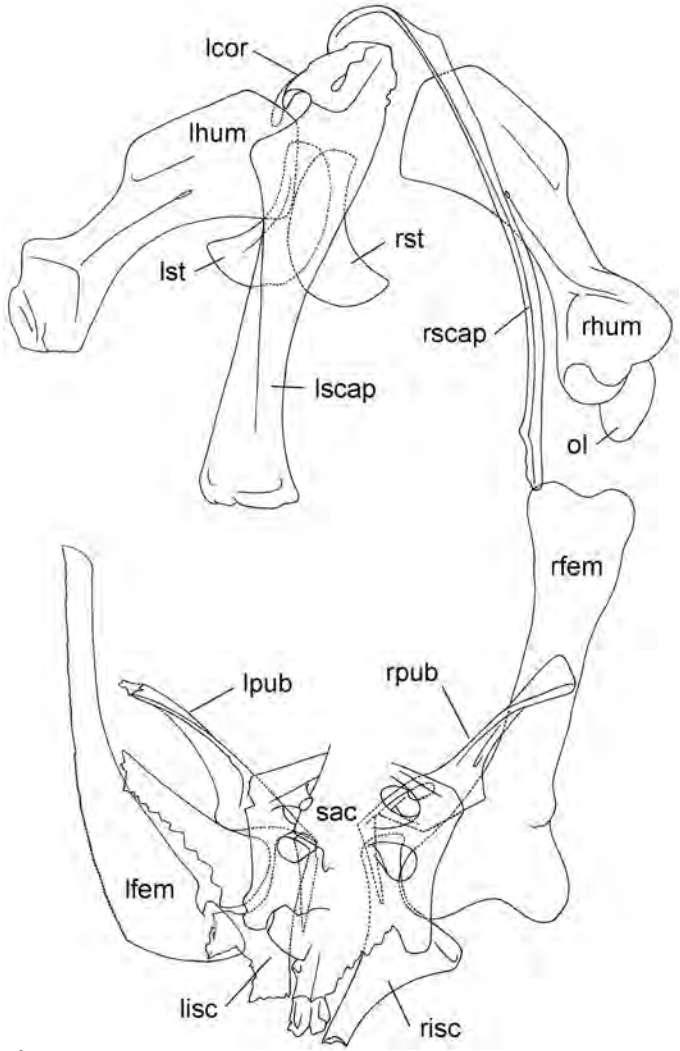

Figure 13. Specimen map for *Vagaceratops irvinensis*, CMN 41357, showing the relative position of limb elements. Adapted and simplified from a map prepared by D. Stoffregen.

Figure 14. Scapulocoracoids. A, right scapulocoracoid in lateral, medial, and posterior views; B, left scapulocoracoid in lateral, medial, and posterior views. *Vagaceratops irvinensis*, CMN 41357.

was also exposed in ventral view. The offset distal end of the metacarpal (at the time assumed to be associated with the pathology) resulted in an extremely unusual orientation of the first digit (Rega et al. 2010) that was hypothesized to represent a 'bunion'—a condition in humans associated with repetitive stress of the first pedal digit. However, in a recent description of an articulated skeleton of *Triceratops* (Fujiwara 2009), it was suggested that not only is the offset distal articular facet a normal feature of the first metacarpal, but that it was oriented distomedially, producing a medial, rather than lateral deflection of the first digit. This suggests that the manus of CMN 41357 was originally reconstructed with the first metacarpal upside down, although it is unclear how, among all of the elements of the closely articulated manus (including the phalanges of the first digit), only the first metacar-

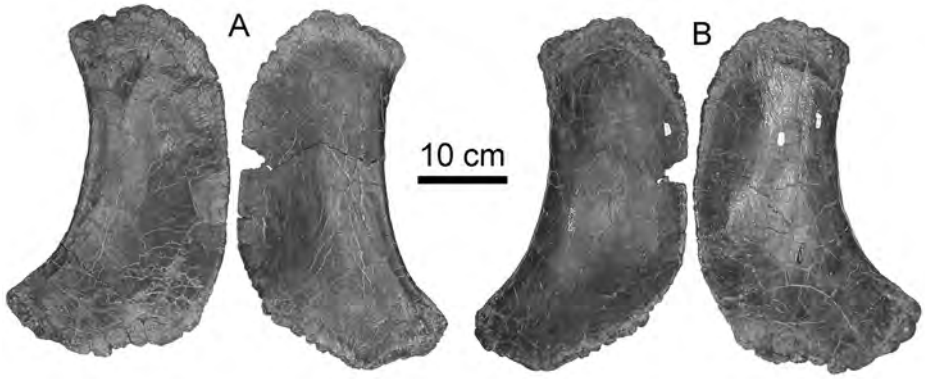

Figure 15. Left and right sternal plates in A, external and B, internal views. *Vagaceratops irvinensis*, CMN 41357.

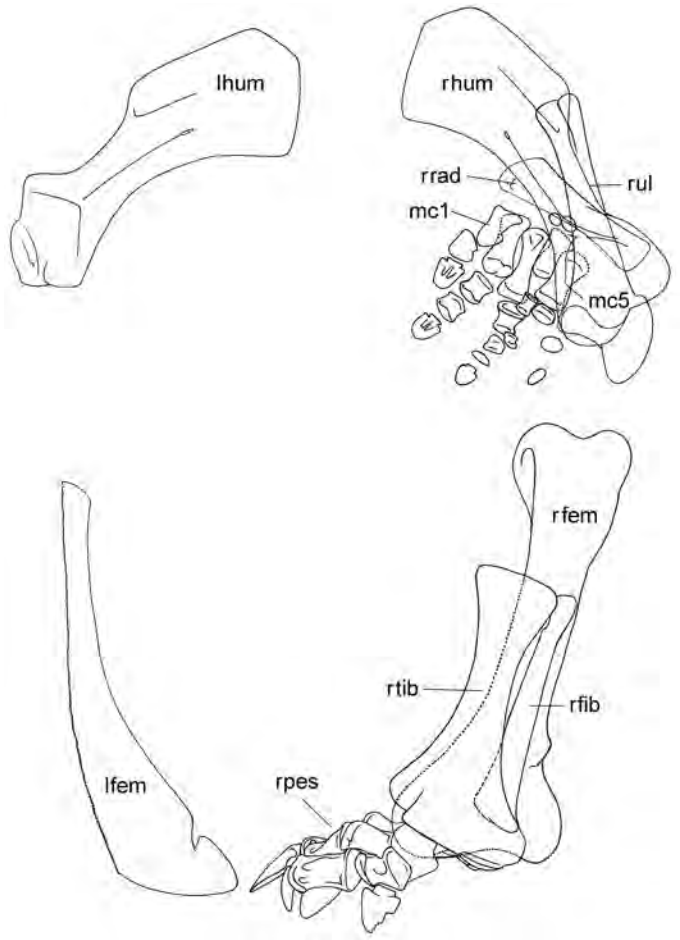

Figure 16. Specimen map showing the relative position of limb elements. Adapted and simplified from a map prepared by D. Stoffregen. *Vagaceratops irvinensis*, CMN 41357.

pal came to be exposed in dorsal view. Regardless, these deformations are consistent with abnormalities produced by repetitive stress injury over long periods of time. This, and the bizarre cauliflower-shaped growths on the cervical vertebrae of CMN 41357 suggest that this individual was quite old when it died.

As in other ceratopsians, the phalangeal formula is 2, 3, 4, 3, 2. The third metacarpal is the largest, indicating that the third digit probably formed the primary axis of the manus. Although the manus is approximately symmetrical around the third digit, the first and second metacarpals and digits are distinctly more robust than those of the fourth and fifth, suggesting only a subsidiary role for the two most lateral digits during locomotion. Only digits 1–3 bear unguals. The terminal phalanx of the fifth digit is much larger and more completely formed (exhibiting an hourglass outline) than that in other ceratopsians (e.g., Brown 1917; Lull, 1933; Brown and Schlaikjer 1940; Fujiwara 2009; Mallon and Holmes 2010; Rega et al. 2010) in which these elements are smaller and oval in outline. Although the distal ends of the terminal phalanges of both digits 4 and 5 bear what appear to be articular facets, no additional phalanges were preserved, and the close articulation of the manus indicates that it is unlikely that any elements were lost during burial. The significance of these facets is therefore uncertain.

Pelvic Girdle and Limb

Neither ilium is preserved in CMN 41357.

Ischium: Both ischia, lacking most of their posteroventral processes, are preserved. The iliac and pubic processes

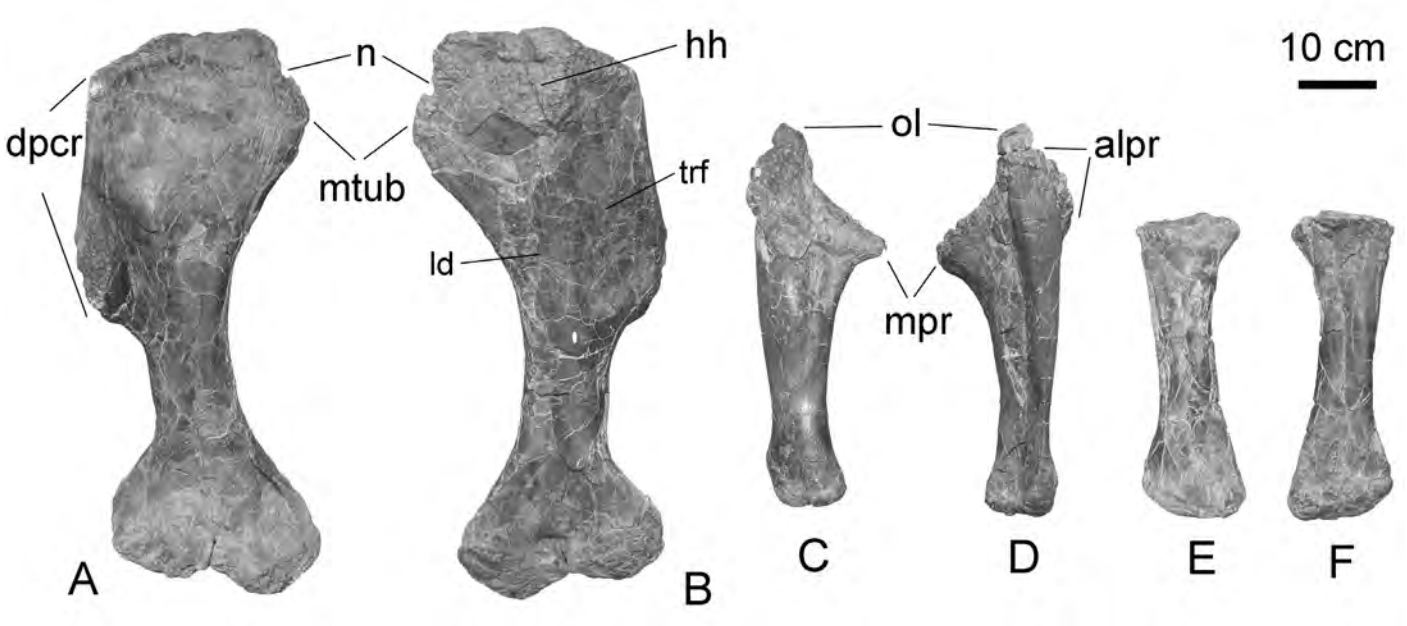

Figure 17. A, B, right humerus in A, flexor (ventral) and B, extensor (dorsal) views; C, D, right ulna in C, anteromedial and D, posterolateral views; E, F, right radius in radius in E, anteromedial and F, posterolateral views. *Vagaceratops irvinensis*, CMN 41357.

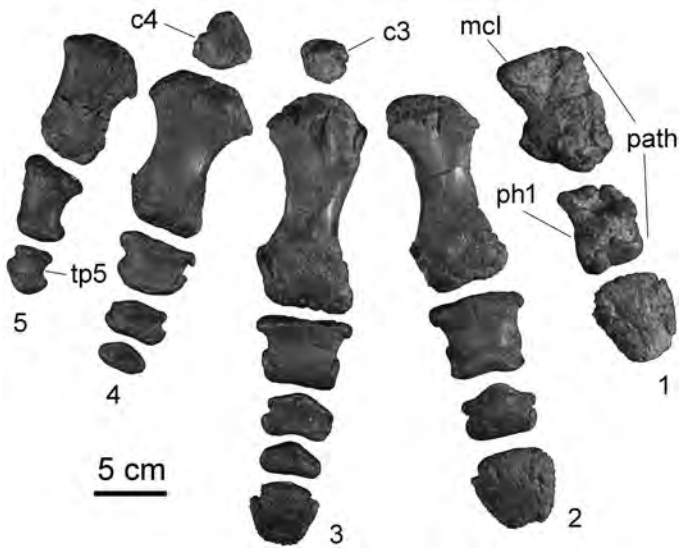

Figure 18. Right manus in dorsal view. *Vagaceratops irvinensis*, CMN 41357.

of the right ischium are complete and undistorted (Fig. 19). The short, fan-shaped iliac process terminates in a broad, convex articular surface for the ilium. The much more elongate pubic process expands anteriorly to form a facet for articulation with the pubis. The curvature of the preserved portion of the acetabular margin suggests that the acetabulum was approximately 170 mm in diameter. The iliac process of the left ischium was damaged during preservation, but the pubic process is well preserved, permitting articulation with the left pubis (Fig. 20B).

Pubis: Both pubes are preserved (Fig. 20), although the distal end of the left prepubic process is incomplete (Fig. 20B). The proximal portion of the flattened shaft of this process is in the frontal (horizontal) plane, but is twisted around its long axis so that its anterior expansion has an oblique orientation, with its internal surface facing dorsolaterally (Fig. 20A). This twisting has not been described in other ceratopsids, although a similar condition has been illustrated for *Centrosaurus* (Lull, 1933:fig. 26). The acetabular region of the pubis forms the cup-shaped anterior portion of the acetabulum (the only part of the joint surface that is ossified). The postpubic process arises as a stout process ventral to the junction of the acetabular and prepubic portions of the bone, and immediately turns posteriorly, forming the ventral border of the large obturator foramen. It extends as a delicate, trough-shaped process that cradles the ventral surface of the ischium. The medial wall of the trough gradually becomes reduced as the process thins posteriorly. The postpubis then turns onto the lateral surface of the ischium and parallels the ventral edge of the ischium for about 120 mm before attenuating to a point (Fig. 20B).

Femur: The left femur was badly weathered and much of it was lost before the specimen was collected (Figs. 1, 16).

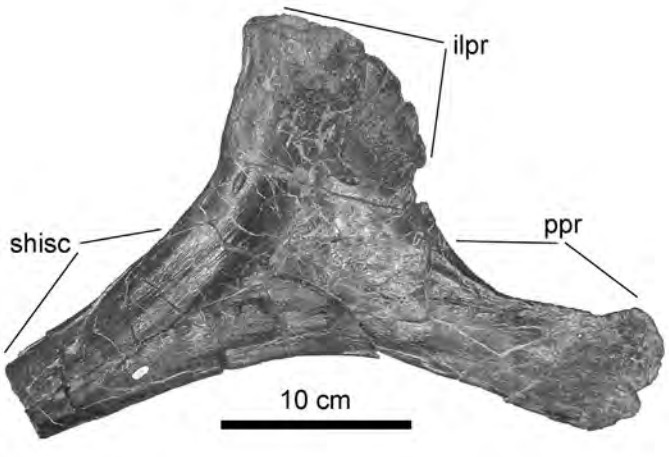

Figure 19. Right ischium, lateral view. *Vagaceratops irvinensis*, CMN 41357.

The right femur is nearly complete (Fig. 21), although most of the greater (lateral) trochanter has been lost to weathering. The maximum length is 760 mm. It appears to be relatively stout compared with those of most other ceratopsids in which the element is described (e.g., Brown 1917; Dodson et al. 2004:fig. 23.7; Holmes and Ryan 2013) except *Triceratops* (Hatcher et al. 1907:fig. 71). This may be an illusion created by postmortem compression. An elongate adductor crest extends proximodistally for the complete length of the posterior (flexor) surface of the shaft. An indistinct swelling, located approximately 40% of the distance to the distal end of the bone, apparently represents the fourth trochanter. This would locate the trochanter in a relatively proximal position in comparison with those of other ceratopsids (Dodson et al. 2004), and protoceratopsids (You and Dodson 2004) in which it is located at about the mid-point of the shaft.

Tibia: The right tibia is complete, but slightly crushed (Fig. 21). It is relatively robust in comparison to those of most other ceratopsids except *Triceratops*. The proximal expansion is damaged and distorted, but the fibular condyle was clearly prominent. The proximal articular surface is in the form of an anteroposteriorly compressed oval. The shaft is quite stout compared to that of other ceratopsids (e.g., *Chasmosaurus*, Maidment and Barrett, 2011; *Centrosaurus*, Lull 1933; *Triceratops*, Hatcher et al. 1907). Distally, the tibia is cupped by a calcaneum laterally and astragalus medially.

The tibia, including the astragalus, is 520 mm in length. The epipodial segment of the rear limb is therefore 68% of the length of the femur, relatively short compared to most ceratopsids (Table 1).

Fibula: The fibula (Fig. 21), other than being relatively robust, is typical of those described for other ceratopsids (e.g., Brown 1917; Lull 1933; Maidment and Barrett 2011; Holmes and Ryan 2013).

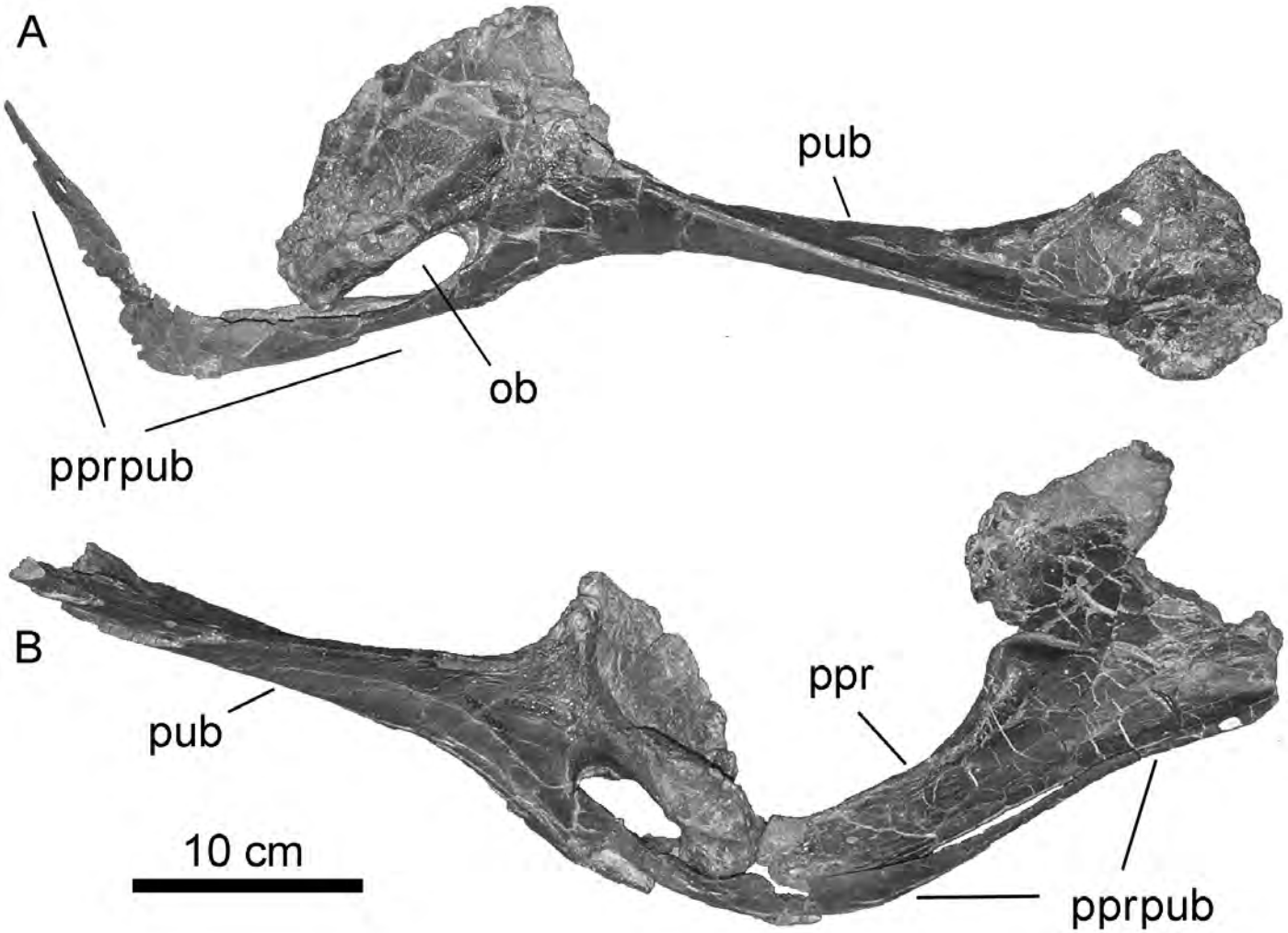

Figure 20. A, right pubis, lateral view; B, left pubis and ischium in articulation, lateral view. *Vagaceratops irvinensis*, CMN 41357.

Tarsus: The right calcaneum remains articulated with the tibia, although a deep furrow between the two bones suggest that co-ossification was incomplete (Fig. 21). The right astragalus (Fig. 21) was preserved slightly disarticulated from the tibia, exposing the coarsely interdigitating matching sutural surfaces that clearly had not co-ossified at the time of death. An additional small element, probably a tarsal (possibly a sesamoid) is preserved immediately proximal to the point of contact of the third and fourth metatarsals and the astragalus and calcaneum (Fig. 22). There is no evidence for the presence of the two large distal tarsal elements described in *Centrosaurus* (Lull 1933). However, during burial, the astagalus and calcaneum were forced downward onto the proximal articular facets of the metatarsals, slightly crushing and 'exploding' the proximal heads of these bones (Fig. 22). It is possible that the tarsals in question may have been crushed into these articular surfaces or otherwise destroyed.

Metatarsus and Pes: The right metatarsus and pes are complete (Fig. 22). The proximal ends of all metatarsals and first phalanges of digits 3 and 4 have suffered some plastic deformation, making meaningful measurements impossible, and portions of the delicate distal margins of the unguals are missing, but otherwise the elements are well preserved. The proximal articular facet of metatarsal I is broadly triangular with its long edge oriented mediolaterally. Metatarsals II, III, and IV have roughly rectangular proximal facets, although the corners are often rounded. The proximal expansions of metatarsals I–IV extensively overlap the proximal facet of its lateral neighbor. Crushing produced when the astragalus and calcaneum were forced into the proximal ends of the metatarsals has probably exaggerated the widths of their proximal heads, and therefore the extent of this overlap. Metatarsals II, III, and IV appear to contact each other distally. Metatarsal V is attached to the proximal end of the lateral side of

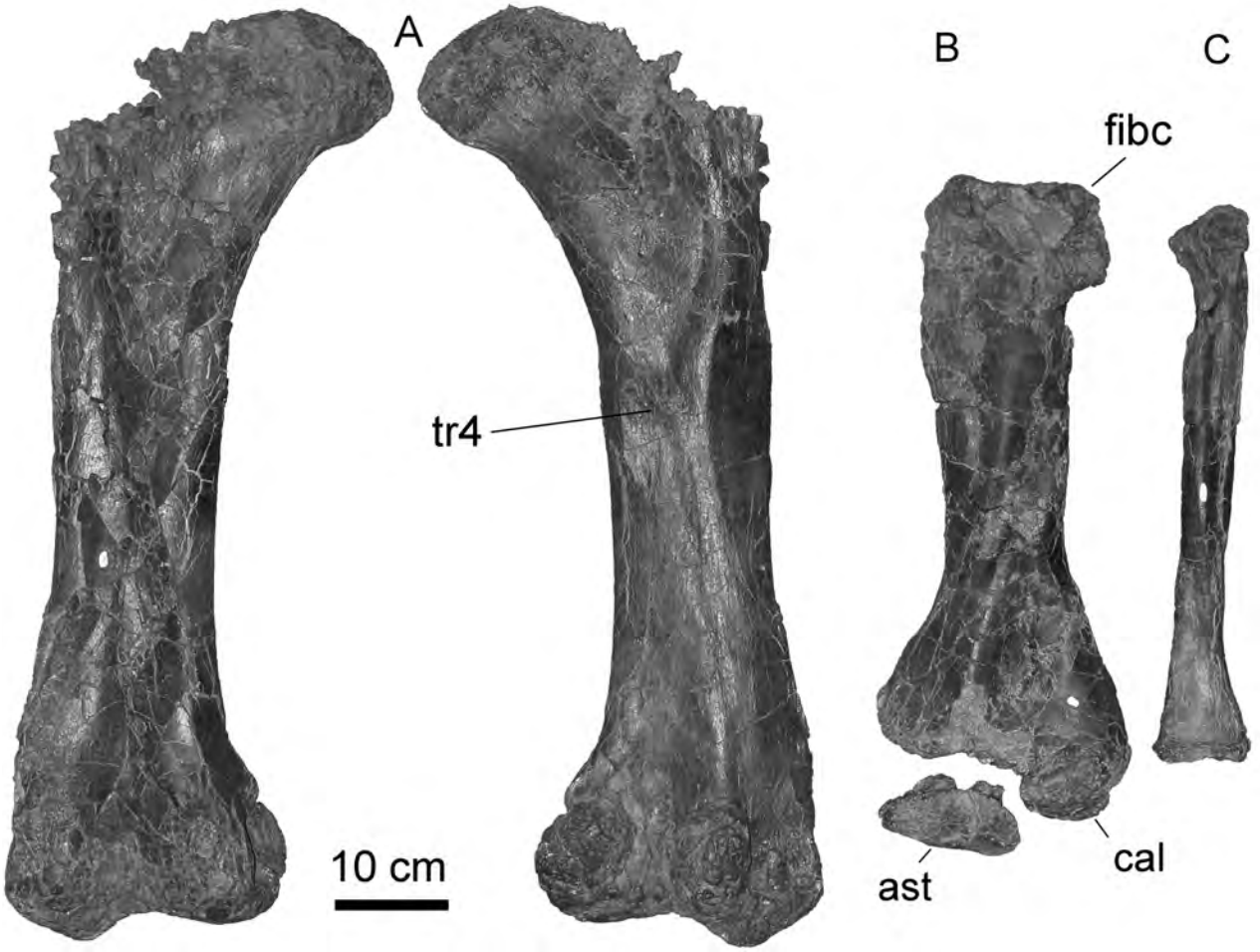

Figure 21. A, right femur in extensor (anterior) and flexor (posterior) views; B, right tibia in flexor (posterior) view. C, right fibula in flexor (posterior) view. *Vagaceratops irvinensis*, CMN 41357.

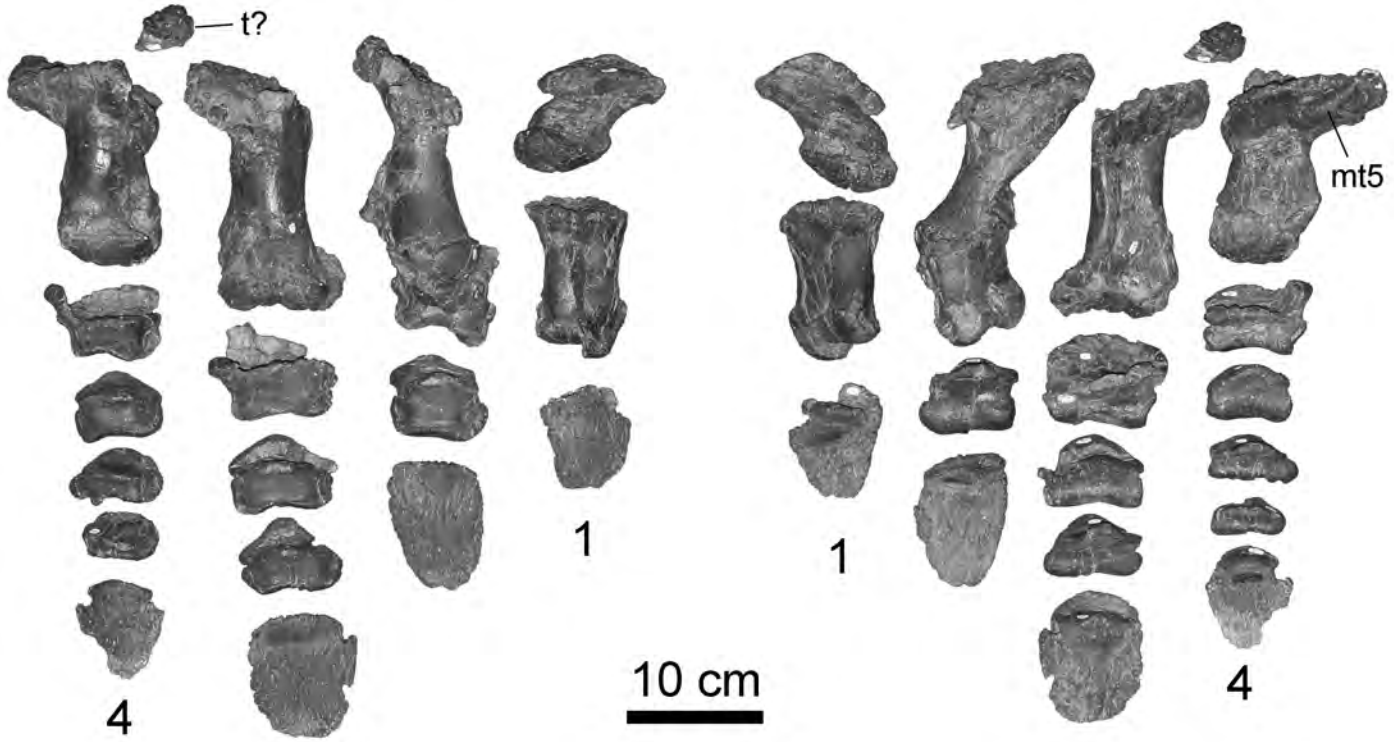

Figure 22. Right pes in dorsal (left) and ventral (right) views. 1, first digit. 4, fourth digit. *Vagaceratops irvinensis*, CMN 41357.

TABLE 1. Ratios of tibia/femur length in ceratopsids based on maximum femur length measured from greater trochanter to lateral condyle; maximum tibia length including astragalus unless otherwise indicated. References cited indicate source of measurements upon which ratios were calculated.

Centrosaurus (Brown 1917)	0.81
Centrosaurus (Lull 1933)	0.70
Styracosaurus (Holmes and Ryan 2013)	0.74
Brachyceratops (Gilmore 1917)	0.80
Avaceratops (Penkalski and Dodson 1999)	0.80*
Triceratops (Gilmore 1917)	0.63
Triceratops (Penkalski and Dodson 1999)	0.59
Triceratops (Fujiwara 2009)	0.66
Vagaceratops	0.68
cf. *Anchiceratops* (Mallon and Holmes 2010)	0.73
Chasmosaurus belli (CMN 2245, Sternberg 1927)	0.71
Chasmosaurus belli (ROM 843, J. Mallon, pers. com.)	0.64
Chasmosaurus cf. *C. belli* (juvenile, UALVP 52613, pers. obs.)	0.85
Pentaceratops (Wiman 1930)	0.74

*astragalus not present

metatarsal IV, and the distal end of the former wraps around onto the flexor surface of the latter (Fig. 22). As in *Centrosaurus* (Brown 1917), metatarsal V is dorsoventrally flattened and curved. Its distal end appears to bear an articular surface, but no phalanges are preserved in association with this element.

Relative proportions of the phalangeal elements resemble those in *Centrosaurus* (Brown 1917; Lull 1933), *Brachyceratops* (Gilmore 1917), and *Styracosaurus* (Holmes and Ryan 2013). As in other ceratopsids, and in contrast with the protoceratopsids *Protoceratops* and *Leptoceratops* (Brown and Schlaikjer 1940:fig. 33), the first phalanx of the first digit is much larger (nearly twice as long) than that of any other digit in the pes. The third digit is the longest despite possessing one less phalanx than the fourth digit. As in other ceratopsids (e.g., Dodson et al. 2004), the size disparity between the shortest digit (digit I) and the longest is distinctly less than in protoceratopsids, and the pes is more nearly symmetrical around the third digit.

DISCUSSION

Articulated ceratopsid postcrania are relatively rare (Holmes and Ryan 2013). As a consequence, the fossil history, and therefore systematics of ceratopsids is based primarily on skull morphology. Recent studies (e.g., Chinnery 2004; Mallon and Holmes 2006; Maidment and Barrett 2011; Holmes and Ryan 2013) have added new data on ceratopsid postcrania. As a result, postcranial characters of potential systematic utility are being identified. In particular, vertebral count, sacrum and rib structure, morphology of the pectoral girdle, humerus, ulna, manus, and femur, as well as propodial/epipodial proportions appear to vary sufficiently in ceratopsids to warrant further attention.

Vertebral Count: Centrosaurines, as far as known, have nine cervical vertebrae, 12 dorsal vertebrae, and one dorsosacral vertebra (Lull 1933). This probably represents the primitive ceratopsian count (Holmes and Ryan 2013). The same count has been reported in some chasmosaurine specimens (e.g., *Chasmosaurus*, CMN 2245; Mallon and Holmes 2006) but not all. One articulated skeleton, usually attributed to cf. *Anchiceratops*, possesses 10 cervicals and 13 additional presacral vertebrae, the latter apparently all pertaining to the dorsal series (Mallon and Holmes 2010). However, the sacrum is highly co-ossified and obscured by the right ilium, and it is not possible to determine the number of dorsosacrals in this specimen. One individual of *Chasmosaurus belli* (ROM 843) has two dorsosacrals in addition to the normal nine cervicals and 12 dorsal vertebrae (Fig. 12), one extra vertebra over the putative primitive number of presacral vertebrae. CMN 41357 is one of the few chasmosaurines (along with ROM 843 mentioned above) that has a complete presacral, dorsosacral and sacral series, permitting an unequivocal count. Like ROM 843, CMN 41357 possesses a second dorsosacral in addition to nine cervicals and 12 dorsals. Unfortunately, there are too few ceratopsids in which a count can be determined to assess whether a phylogenetic pattern exists. The fact that at least three individuals among a fairly small set of skeletons possess supernumerary presacral vertebrae suggests that they are not anomalous. However, other than the fact that extra vertebrae only appear to occur in chasmosaurines, no specific hypotheses regarding the phylogenetic significance of presacral/dorsosacral vertebral count are possible at this point.

Mid-ventral Groove on Sacrum: As far as known, chasmosaurines possess a conspicuous longitudinal midventral groove on the sacrum. Centrosaurines also have such a groove, but it is much more shallow (Maidment and Barrett 2011). This groove is certainly present in CMN 41357 (Fig. 11), but its precise length and depth cannot be measured accurately, as the specimen is presently on exhibit, and is not accessible.

Rib Morphology: The morphology of the cervical and dorsal ribs of CMN 41357 transitions from long and relatively straight anteriorly to broadly curved in the mid-thorax, to relatively short and strongly curved in the posterior portion of the trunk, reflecting the narrow, deep anterior portion of the chest and wider, but shallower posterior chest and abdomen. This morphology is common to all known ceratopsids (e.g., Brown, 1917; Lehman 1989; Holmes and Ryan, 2013). However, morphology of the ribs associated with the last dorsal and dorsosacral vertebrae

appears to vary. The ribs associated with the last dorsal vertebra are relatively straight, and project laterally and curve gently anteriorly, paralleling the curved inner surface of the anterior iliac blade. Essentially the same morphology occurs in *Styracosaurus* (Holmes and Ryan 2013) and *Chasmosaurus belli* (ROM 843, Fig. 12). *Centrosaurus* also shows a similar morphology (Lull 1933), although the last dorsal vertebra appears to have been interpreted as the first dorsosacral by Lull (1933:fig. 18), and Brown (1917) makes no mention of this morphology in the description of another specimen of this taxon. Whether this indicates a real difference between the two specimens, or simply the result of incomplete preservation is unknown. There is no doubt that some variability in rib morphology occurs in the dorsosacral region. The dorsosacral vertebrae of ceratopsids typically lack separate ribs, but rather articulate directly with the dorsomedial edges of the ilia by way of laterally directed, spatulate transverse processes (e.g., Lull 1933;fig. 17). However, in CMN 41357, the transverse processes of DS1 resembles those of D12 in being rectangular in dorsal outline, and unlike those of DS2, do not articulate with the ilia. Rather, each process bears a long, blade-like rib that projects anterolaterally (Fig. 9). Unlike the 12th dorsal rib, it lacks a capitulum, and is fused to the end of its transverse process. It is not known how common this morphology is, as this portion of the ceratopsid skeleton is rarely exposed or preserved. However, in ROM 843 (*Chasmosaurus belli*), the latter morphology is exhibited not only by the ribs of DS1, but also D12, the latter of which are usually 'free' ribs (Fig. 12). Both sets of ribs project anterolaterally, paralleling the curvature of the medial surface of the ilium. The ribs of D12 articulate with the ilium only distally, the ribs of DS1 articulate with the ilium throughout most of their lengths. All of this suggests that rib morphology in the first dorsosacral segment (the possibly last dorsal segment) is labile, and can shift anteriorly or posteriorly, possibly in response to the length and position of the adjacent iliac blade, but a phylogenetic signal has yet to be identified.

Width of Sternal Plates: The sternal plates of CMN 41357 are noticeably wider than those of most other ceratopsids. The significance of this is unclear. The perimeter of a sternal plate was presumably extended in cartilage, and so an estimation of the size and shape of the entire structure based on its ossified portion can only be approximate. Sternal plates have been described in only a few ceratopsids (*Centrosaurus*, Brown 1917, Lull 1933; *Styracosaurus*, Holmes and Ryan 2013; *Chasmosaurus*, Mallon and Holmes, 2006; *Triceratops*, Brown 1906). Limited evidence suggests that there is considerable interspecific variability (e.g., Mallon and Holmes 2006), but more data are needed before it can be determined if this has any phylogenetic utility.

Scapula Morphology: Centrosaurines, as far as known, possess a small acromion process that is restricted to the anterior-most portion of the dorsal edge of the scapular blade, while in chasmosaurines, the process is more extensive, extending further posteriorly on the scapular blade (Maidment and Barrett 2011). CMN 41357 clearly exhibits the chasmosaurine morphology, supporting the hypothesized morphological dichotomy between the two subfamilies.

The dorsalis scapulae ridge on the lateral scapular surface is somewhat variable in ceratopsids, but generally arises on the proximoventral corner of the scapular blade, and trends diagonally to its distal termination at or near the dorsal margin of the blade. The only known exceptions are *Triceratops* and *Torosaurus*, in which the ridge extends up the scapular blade midway between its dorsal and ventral edges. Although these two morphologies do not appear to separate centrosaurines and chasmosaurines, the latter morphology may distinguish *Triceratops* and *Torosaurus* from all other ceratopsids.

Humerus Morphology: Chasmosaurines and centrosaurines appear to have distinct humerus morphologies (Chinnery 2004; Maidment and Barrett 2011). In chasmosaurines, the medial tuberosity is set off from the dorsal surface of the humerus by a distinct notch (Maidment and Barrett 2011), whereas in centrosaurines, this notch is at best only poorly developed (e.g., Holmes and Ryan 2013:fig. 19). In chasmosaurines, the deltopectoral crest extends to the mid-length of the humerus, whereas in centrosaurines, it does not extend as far distally. In addition, the proximal humeral expansion in chasmosaurines is larger and distinctly rectangular in outline with a straight, or even slightly convex preaxial border when viewed in flexor aspect (e.g., Mallon and Holmes 2010:figs. 13.6, 13.7; Maidment and Barrett 2011:fig. 23). In centrosaurines as far as known, the proximal humeral expansion is smaller, narrows proximally, and has a gently concave preaxial border (e.g., Lull 1933:fig. 21; Holmes and Ryan 2013:fig. 19). The insertion point for the latissimus dorsi is prominently marked. In all of these features, the humerus of *Vagaceratops* conforms to the morphology attributed to chasmosaurines.

Ulna Morphology: In chasmosaurines, the ulna bears a prominent medial process and strongly concave trochlear notch. In centrosaurines, as far as known, the process is less prominent, the trochlear notch is distinctly less concave, and the olecranon is relatively shorter (e.g., Lull 1933:fig. 22; Holmes and Ryan 2013:fig. 20). However, this feature has only been described in a few centrosaurines, and more data are required to confirm these apparent differences.

Humerus-Epipodial Proportions: The epipodium of CMN 41357, at only 54% of the length of the humerus,

is relatively short compared with those of other ceratopsids for which this ratio has been established. These proportions, along with the robust morphology of the humerus, suggest that the forelimb of *Vagaceratops* was adapted for weight bearing and/or a powerful step cycle. Whether relative epipodial length has any utility in separating chasmosaurines and centrosaurines, however, is uncertain. The ratio in *Centrosaurus*, as measured in several articulated skeletons, averages about 0.60 (P.J. Currie, pers. com. 2013). Although data for other centrosaurines are less plentiful, the ratio in *Styracosaurus* and *Pachyrhinosaurus* (measured from a single specimen in each case), is 0.63 (Holmes and Ryan 2013; P.J. Currie, pers. com. 2013). Although *Vagaceratops* and some other chasmosaurines (e.g., cf. *Anchiceratops*) arguably have distinctly shorter front limb epipodials, in others (e.g., *Pentaceratops* and *Triceratops*), the epipodials are as long as or longer than those of centrosaurines. However, ceratopsid forelimb anatomy is not well documented, and consequently this ratio unknown, in many ceratopsid taxa; more data are needed.

Manus Morphology: Other than *Vagaceratops*, a complete manus is unknown in ceratopsids except for *Centrosaurus* (Brown 1917; Lull 1933), *Chasmosaurus* (Rega et al. 2010), cf. *Anchiceratops* (Mallon and Holmes 2010), and *Triceratops* (Fujiwara 2009). Given a sample size of five taxa, any discussion of potentially significant differences in manus structure is certainly premature. However, it is still worth noting the unusual morphology of the terminal phalanges of the fourth and fifth digits of *Vagaceratops*. In all other ceratopsids that preserve a manus, as well as the more basal ceratopsians *Protoceratops* and *Leptoceratops* (Brown and Schlaikjer 1940), these elements are poorly formed nubbins. In *Vagaceratops*, they are well-formed with what appear to be articular surfaces on both proximal and distal surfaces. The terminal phalanx of the fifth digit is also relatively large with a distinct 'waisted' shaft between its proximal and distal facets. The admittedly limited distribution of these features in ceratopsians suggests that *Vagaceratops* may be derived with respect to this character, but the condition in more taxa must be established before more can be said.

Femur Morphology: In ceratopsids and protoceratopsids, the fourth trochanter is generally positioned midway between the proximal and distal ends of the femur. In *Vagaceratops*, it is noticeably closer to the proximal end. The proximally placed fourth trochanter suggests the capacity for relatively rapid step cycle, which is at odds with distally placed pectoralis insertion on the humerus and short epipodials of the front limbs. However, the rear limbs of *Vagaceratops*, as in other ceratopsids, were certainly fully parasagittal in orientation. In contrast, the forelimb posture was at best only partially parasagittal. The humerus never deviated very much from the horizontal throughout the step cycle, and the elbows were distinctly flexed (Thompson and Holmes 2007). Given the very different kinematics resulting from the fore- and hind limb postures, it is possible that the position of the muscle insertions and proportions of the hind limb were not as constrained as those of the front limbs, allowing them to deviate from a stance dominated by weight-bearing demands. This could be of taxonomic significance, but if so, the currently known distribution of this character suggests that the condition in *Vagaceratops* is apomorphic. Alternately, the condition in *Vagaceratops* may simply reflect some biomechanical constraint. Perhaps significantly, the small (and probably juvenile) *Brachyceratops* also has a relatively proximally placed fourth trochanter.

Propodial/Epipodial Proportions: Based on measurements from preserved skeletons and previously published data, it is possible to estimate the relative lengths of the propodial and epipodial segments of the hind limb of a number of ceratopsids by calculating the tibial length/femoral length (Table 1). *Vagaceratops* falls at the low end of the range for ceratopsids. Although this ratio shows considerable variability in ceratopsids, there is no convincing evidence that chasmosaurine and centrosaurine ceratopsids can be separated on the basis of these limb proportions. Although the centrosaurines listed in Table 1 have, on average, longer hind limb epipodials than do the chasmosaurines, it would be imprudent to read too much into this. There is considerable variability in limb proportions in the family, and in taxa for which more data is available (e.g., *Centrosaurus*, *Triceratops*), there is considerable intrageneric variability. Partly as a consequence, values in the two subfamilies overlap. Furthermore, there appears to be an ontogenetic and/or size effect. Small (and/or juvenile) individuals (e.g., *Brachyceratops*, *Avaceratops*, a juvenile *Chasmosaurus* cf. *C. belli*) score at the high end of the range, while the large *Triceratops* scores at the low end. Although propodial/epipodial proportions in protoceratopsids (e.g., Brown and Schlaikjer 1940, 1942) indicate that a relatively high tibial/femoral ratio (>1.0) is primitive for ceratopsians, it has not yet been possible to demonstrate an evolutionary trajectory with respect to this character within the Ceratopsidae.

SUMMARY

This, and other recent studies (Chinnery 2004; Maidment and Barrett 2011) confirm that variation does exist in the postcranial skeleton of ceratopids. Some of this variation is almost certainly of taxonomic utility. Some features (e.g., details of the acromion process, humerus and ulna morphology) support the existence of two families,

Centrosaurinae and Chasmosaurinae, a previously well-established hypothesis based on cranial anatomy. With the exceptions of the course of the supracoracoideus ridge on the scapula, which appears to be a synapomorphy of *Triceratops* and *Torosaurus*, other anatomically variable features within the family show no obvious congruence with a centrosaurine-chasmosaurine dichotomy or suggest any other taxonomic arrangement. Other possible causes of this variability include species apomorphies, intraspecific variation or random variation at the family level, sexual dimorphism, or allometry. The significance of this variation can only be clarified through the discovery and description of more ceratopsid postcranial skeletons representing a wider range of taxa.

ACKNOWLEDGEMENTS

Thanks to D. Stoffregen, C. Kennedy, and C. Qiang for expert preparation of the specimen, M. Burns, V. Arbour, and N. Campione for discussions about ribs of ornithischian dinosaurs, E. Rega for discussions on bone pathologies, and M. Ryan for discussions about ceratopsids in general. J. Mallon and P. J. Currie provided measurements of ceratopsid elements. In particular, I thank B. Chinnery-Allgeier, S. Maidment, and J. Mallon for helpful critiques and editorial comments.

LITERATURE CITED

Adams, D.A. 1988. Structure and function of the ceratopsian forelimb, PhD dissertation, University of California, Berkeley, 379 pp.

Brown, B. 1906. New notes on the osteology of *Triceratops*. Bulletin of the American Museum of Natural History 22:297–301.

Brown, B. 1917. A complete skeleton of the horned dinosaur *Monoclonius*, and a description of a second skeleton showing skin impressions. Bulletin of the American Museum of Natural History 37:281–306.

Brown, B., and E.M. Schalikjer 1940. The structure and relationships of *Protoceratops*. Annals of the New York Academy of Sciences 40:133–266.

Brown, B., and E.M. Schalikjer. 1942 The skeleton of *Leptoceratops* with the description of a new species. American Museum Novitates, 1169:1–15.

Campione, N., and R. Holmes. 2006. The anatomy and homologies of the ceratopsid syncervical. Journal of Vertebrate Paleontology 26:1014–1017.

Chinnery, B. 2004. Morphometric analysis of evolutionary trends in the ceratopsian postcranial skeleton. Journal of Vertebrate Paleontology 24:591–609.

Currie, P.J., W. Langston Jr., and D.H. Tanke. 2008. A New Horned Dinosaur from an Upper Cretaceous Bone Bed in Alberta. NRC Research Press, Ottawa, Ontario, Canada, 144 pp.

Dodson, P., C.A. Forster, and S.D. Sampson. 2004. Ceratopsidae; pp. 494–513 in D.B. Weishampel, P. Dodson, and H. Osmólska (eds.), The Dinosauria, second edition, University of California Press, Berkeley, California.

Fujiwara, S-I. 2009. A reevaluation of the manus structure in Triceratops (Ceratopsia: Ceratopsidae). Journal of Vertebrate Paleontology 29:1136–1147.

Gilmore, C.W. 1917. *Brachyceratops*, a ceratopsian dinosaur from the Two Medicine Formation of Montana. United States Geological Survey Professional Paper 103:1–45.

Hatcher, J.B., O.C. Marsh, and R.S. Lull. 1907. The Ceratopsia. United States Geological Survey Monograph 49:1–300.

Holmes, R.B, and C. Organ. 2007. An ossified tendon trellis in *Chasmosaurus* (Ornithischia: Ceratopsidae). Journal of Paleontology 81:411–414.

Holmes, R. and M.J. Ryan. 2013. The postcranial skeleton of *Styracosaurus albertensis*. Kirtlandia 58:5–37.

Holmes, R.B., C. Forster, M. Ryan, and K.M. Shepherd. 2001. A new species of *Chasmosaurus* (Dinosauria: Ceratopsia) from the Dinosaur Park Formation of southern Alberta. Canadian Journal of Earth Sciences 38:1423–1438.

Johnson, R.E. and J.H. Ostrom. 1995. The forelimb of *Torosaurus* and an analysis of the posture and gait of ceratopsian dinosaurs; pp. 205-218 in J.J. Thomason, Functional Morphology in Vertebrate Paleontology.Cambridge University Press, Cambridge, U.K.

Lehman, T.M. 1989. *Chasmosaurus mariscalensis*, sp. nov., a new ceratopsian dinosaur from Texas. Journal of Vertebrate Paleontology 9:137−162

Lehman, T.M. 1998. A gigantic skull and skeleton of the horned dinosaur *Pentaceratops sternbergi* from New Mexico. Journal of Paleontology 72:894–906.

Longrich, N.R. 2014. The horned dinosaurs *Pentaceratops* and *Kosmosaurus* from the upper Campanian of Alberta and implications for dinosaur biogeography. Cretaceous Research 51:292−308.

Lull, R. S. 1933. A revision of the Ceratopsia or horned dinosaurs. Memoires of the Peabody Museum of Natural History 3:1–175.

Mallon, J.C., and R.B. Holmes. 2006. A reevaluation of sexual dimorphism in the postcranium of the chasmosaurine ceratopsid *Chasmosaurus belli* (Dinosauria: Ornithischia). The Canadian Field-Naturalist 120:403—412.

Mallon, J.C., and R. Holmes. 2010. Description of a complete and fully articulated chasmosaurine postcranium previously assigned to *Anchiceratops* (Dinosauria: Ceratopsia); pp. 189–202 in M.J. Ryan, B.J. Chinnery-Allgeir, and D.A. Eberth (eds.), New Perspectives on Horned Dinosaurs: The Royal Tyrrell Museum Ceratopsian Symposium. University of Indiana Press.

Mallon, J.C., R. Holmes, J.S. Anderson, A.A. Farke, and D.C. Evans. 2014. New information on the rere horned dinosaur *Arrhinoceratops brachyops* (Ornithischia: Ceratopsidae) from the Upper Cretaceous of Alberta, Canada. Canadian Journal of Earth Sciences 51:618-634.

Maidment, S.C.R. and P.M. Barrett. 2011. A new specimen of *Chasmosaurus belli* (Ornithischia: Ceratopsidae), a revision of the genus, and the utility of postcrania in the taxonomy and systematics of ceratopsid dinosaurs. Zootaxa 2963:1–47.

Penkalski, P. and P. Dodson. 1999. The morphology and systematics of *Avaceratops*, a primitive horned dinosaur from the Judith River

Formation (Late Campanian) of Montana, with a description of a second skull. Journal of Vertebrate Paleontology 19:692–711.

Rega, E., R. Holmes, and A. Tirabasso. 2010. Habitual locomotor behavior inferred from manual pathology in two late Cretaceous chasmosaurine dinosaurs, *Chasmosaurus irvinensis* and *Chasmosaurus belli* (ROM 843); pp. 340–354 in M. J. Ryan, B. J. Chinnery-Allgeier, and D. A. Eberth (eds.), New Perspectives on Horned Dinosaurs. Indiana University Press, Bloomington and Indianapolis.

Sampson, S.D., and M.A. Loewen. 2010. Unraveling a radiation: a review of the diversity, stratigraphic distribution, biogeography, and evolution of horned dinosaurs (Ornithischia: Ceratopsidae); pp. 405–427 in M.J. Ryan, B.J. Chinnery-Algeier, and D.A. Eberth (eds.), New Perspectives on Horned Dinosaurs. Indiana University Press, Bloomington, Indiana.

Sampson, S., M.A. Loewen, A.A. Farke, E.M. Roberts, C.A. Forster, J.A. Smith, and A.L. Titus. 2010. New horned dinosaurs from Utah provide evidence for intracontinental dinosaur endemism. PLoS One 5(9):1–11.

Sternberg, C.M. 1927. Horned dinosaur group in the National Museum of Canada. The Canadian Field Naturalist 41:67–73.

Thompson, S. and R. Holmes. 2007. Forelimb stance and step cycle in *Chasmosaurus irvinensis* (Dinosauria: Neoceratopsia). Palaeontologia Electronica 10(1):5A:17 p.

Tsuihiji, T. and P. Makovicky. 2007. Homology of the neoceratopsian cervical bar elements. Journal of Paleontology 81:1132–1138.

Wiman, C. 1930. Über Ceratopsia aus der Oberen Krreide in New Mexico. Nova Acta Regiae Societatis Scientiarum Upsaliensis (ser. 4) 7(2):1–19, 7 plates.

You, H. and P. Dodson. 2004. Basal Ceratopsia; pp. 478–493 in D.B. Weishampel, P. Dodson, and H. Osmólska (eds.), The Dinosauria, second edition, University of California Press, Berkeley, California.

Appendix 1. Measurements of *Vagaceratops irvinensis,* CMN 41357.

Measurements of limbs and girdles (in mm).

Scapula (left)	
Total length	750
Glenoid length	121
Minimum shaft width	111
Maximum width at glenoid	210
Coracoid (right)	
Scapular suture length	135
Maximum anteroposterior width	242
Sternal plate (left)	
Length	310
Anterior width from midline	137
Posterior width from midline	188
Sternal plate (right)	
Length	304
Anterior width from midline	125
Posterior width from midline	201
Humerus (right)	
Total length	610
Proximal end to distal corner of deltopectoral crest	320
Maximum diameter of proximal articular condyle	98
Width of proximal expansion at mid-length	182
Minimum shaft width in extensor aspect	90
Minimum shaft circumference	247
Width of distal expansion	225
Ulna (right)	
Total length including olecranon	410
Maximum width of proximal expansion	154
Maximum width of proximal expansion (extensor–flexor)	110
Maximum width of distal expansion	79
Minimum shaft width in extensor aspect	56
Radius (right)	
Maximum length	340
Proximal width	112
Distal width	114
Minimum shaft diameter in extensor aspect	61
Right Pubis	
Length (excluding posterior process)	427
Width of distal end of prepubic process	109
Maximum width of acetabular contribution	160
Minimum width of prepubis	51
Length of postpubic process (from obturator foramen)	211
Left Pubis	
Length (excluding posterior process)	—
Width of distal end of prepubic process	—
Maximum width of acetabular contribution	117
Minimum width of prepubis	61
Length of postpubic process (from obturator foramen)	233
Ischium (right)	
Distance from proximal end of iliac process to distal end of pubic process	282
Minimum shaft width	46
Femur (right)	
Maximum length	760
Minimum shaft diameter in flexor aspect	126
Minimum shaft circumference	344
Mediolateral width of distal expansion	208
Mediolateral width of proximal expansion (incl. head) (estimated)	259
Anteroposterior depth of proximal expansion	49
Anteroposterior depth of distal expansion	86
Tibia (right)	
Length	520
Width of proximal expansion	174
Shaft diameter at mid-length	103
Width of distal expansion	240
Fibula (right)	
Length	490
Maximum width of proximal expansion	71
Minimum shaft width	43
Maximum width of distal expansion	105

Measurements of right metacarpus and manus (in mm)

	Length	Proximal width	Distal width
Metacarpals			
I	87	65	60
II	135	61	64
III	145	69	69
IV	107	75	60
V	86	59	47
Phalanges (excluding unguals)			
I(1)	60	49	47
II(1)	54	64	50
II(2)	36	50	48
III(1)	47	64	52
III(2)	30	45	46
III(3)	23	40	34
IV(1)	37	53	47
IV(2)	24	38	41
IV(3)	18	32	30
V(1)	54	43	34
V(2)	30	26	30

Unguals	Length	Proximal condyle width	Proximal condyle height
1	59	45	—
2	59	46	22
3	44	34	18

Measurements of right metatarsus and pes (in mm)

	Length	Proximal width	Distal width
Metatarsals			
I	104	90	72
II	187	94	68
III	180	97	94
IV	148	112	76
V	72	32	25
Phalanges (excluding unguals)			
I(1)	119	76	67
II(1)	90	68	68
II(2)	50	65	68
III(1)	65	86	83
III(2)	54	76	72
III(3)	47	61	70
IV(1)	54	76	65
IV(2)	40	59	61
IV(3)	32	65	65
IV(4)	27	52	54

Unguals	Length	Proximal condyle width	Proximal condyle height
1	81	49	42
2	92	57	35
3	91	63	39
4	73	44	27